Zoological Journal of the Linnean Society, 2024, XX, 1–17
https://doi.org/10.1093/zoolinnean/zlae039
Advance access publication 24 April 2024
Original Article

Original Article

Systematics and biogeography of a Sunda-Papuan snake lineage (Natricidae: *Tropidonophis* Jan 1863)

Jackson R. Roberts[1–3,*], Fred Kraus[4], Allen Allison[5], Stephen J. Richards[6], Bulisa Iova[7], Burhan Tjaturadi[8], Sara Ruane[9], Christopher C. Austin[1,2]

[1]Division of Herpetology, Museum of Natural Science, Louisiana State University, Baton Rouge, Louisiana, 70803, United States
[2]Department of Biological Sciences, Louisiana State University, Baton Rouge, Louisiana, 70803, United States
[3]Sternberg Museum of Natural History, Fort Hays State University, Hays, Kansas, 67601, United States
[4]Department of Ecology and Evolutionary Biology, University of Michigan, Ann Arbor, Michigan, 48109, United States
[5]Department of Natural Science, Bernice P. Bishop Museum, Honolulu, Hawaii, 96817, United States
[6]Department of Herpetology, South Australian Museum, Adelaide, SA, 5000, Australia
[7]Papua New Guinea National Museum and Art Gallery, Boroko, National Capital District, Papua New Guinea
[8]Center for Environmental Studies, Sanata Dharma University (CESSDU), Yogyakarta, Indonesia
[9]Life Sciences Section, Negaunee Integrative Research Center, Field Museum of Natural History, Chicago, Illinois, 60605, United States

[*]Corresponding author. Zoology Division, Sternberg Museum of Natural History, 3000 Sternberg Drive, Hays, Kansas 67601. E-mail: jrroberts6@fhsu.edu

ABSTRACT

Sunda-Papuan keelback snakes (Serpentes: Natricidae: *Tropidonophis* Jan 1863) include 20 species distributed from the Philippines south-east through the Moluccas to New Guinea and Australia. Diversity of this insular snake lineage peaks on the island of New Guinea. Previous phylogenetic studies incorporating *Tropidonophis* have been limited to multi-locus Sanger-sequenced datasets with broad squamate or family-level focus. We used a targeted-sequence capture approach to sequence thousands of nuclear ultraconserved elements (UCEs) to construct the most comprehensive sequence-based phylogenetic hypothesis for this genus and estimate ancestral biogeography. Phylogenies indicate the genus is monophyletic given recent taxonomic reassignment of *Rhabdophis spilogaster* to *Tropidonophis*. All UCE phylogenies recovered a monophyletic *Tropidonophis* with reciprocally monophyletic Philippine and New Guinean clades. Divergence dating and ancestral range estimation suggest dispersal to New Guinea from the Philippines to have occurred during the Mid-Miocene via the Oceanic Arc Terranes. From Late Miocene into the Pliocene the genus experienced rapid diversification from orogeny of the New Guinean Central Cordillera from Oceanic Arc Terrane accretion on the northern boundary of the Sahul Shelf. Future collecting of missing taxa from the Moluccas and Indonesian Papua will better the understanding of non-volant faunal biogeography and diversification in this tectonically complex Pacific arena.

Keywords: biogeography; herpetology; Oceania; Pacific; systematics; taxonomy

INTRODUCTION

Wallace's, Lydekker's, and Weber's Lines are among the most examined and well-known biogeographic divides, demarcating the barriers of faunal turnover of the Sunda Shelf, the Sahul Shelf, and the point of faunal intermediacy (Wallace 1860, Lydekker 1896, Mayr 1944, Simpson 1977, Brown 2016). The Sunda-Papuan region of the Pacific has provided a complicated and fascinating area for biogeographers to hypothesize and contemplate floral and faunal dispersal and speciation due to the complex tectonic history of the region, especially that of New Guinea, with its tectonic affiliation with Australia and geographic proximity to Wallacea. Biogeographers have examined these demarcations for years to assess their permeability, with the overall conclusion that these biogeographic barriers are much more porous than originally thought, even to non-volant terrestrial fauna (Flannery 1990, Clouse and Giribet 2007, Weijola *et al.* 2019, Karin *et al.* 2020).

To say disagreement exists regarding the tectonic and geologic history of New Guinea is an understatement (Hall 2002, Quarles van Ufford and Cloos 2005, Polhemus 2007, Holm, Rosenbaum and Richards 2016). In short, New Guinea is the topographically complex northern margin of the Australian Plate that collided with the south-western margin of the Pacific Plate. Discrepancy between models exists in the proposed timing of orogenic

Received 26 June 2023; revised 19 February 2024; accepted 12 March 2024

events, but agreement exists regarding the primary types of tectonic events that created New Guinea: continental plate collision (Australian and Pacific) and multiple instances of island arc accretion (Hamilton 1979, Pigram and Davies 1987, Hall 2002, Hill and Hall 2003, Quarles van Ufford and Cloos 2005, Baldwin *et al.* 2012). The tectonic regions of New Guinea comprise the Australian Craton (southern third of New Guinea), East Papua Composite Terrane (EPCT; south-eastern Papuan Peninsula), Fold Belt (the Central Cordillera), and the Oceanic Arc Terranes (northern third of New Guinea) (Polhemus 2007, Slavenko *et al.* 2020, Hill *et al.* 2023). Some workers have treated the Vogelkop ('Bird's Head') as a separate tectonic zone (Hill *et al.* 2023), but despite its unique history, the Vogelkop comprises continental crust that broke away from the Australian Craton (Pigram and Davies 1987, Polhemus 2007).

Evolutionary biologists working with New Guinean fauna commonly reference two of the many tectonic hypotheses for estimating ancestral biogeography: Hall (2002) and Quarles van Ufford and Cloos (2005) (Unmack *et al.* 2013, Toussaint *et al.* 2014, Slavenko *et al.* 2020, Tallowin *et al.* 2020). Hall (2002) recognized four primary tectonic events that formed New Guinea: at 50 Mya, the emplacement of the Papuan ophiolite (EPCT), at 45 Mya, the emplacement of the Sepik ophiolites along the northern margin of the Australian plate and creation of the East Caroline Arc north of New Guinea, at 18 Mya, formation of the Maramuni Arc by subduction of the Solomon Sea plate, and at 5 Mya, clockwise rotation and southward migration of the East Caroline Arc resulting in the accretion of arc terranes along the northern margin of the Australian plate, creating significant uplift of both the northern coast of New Guinea and Fold Belt (Central Cordillera) (Fig. 1).

Quarles van Ufford and Cloos (2005) suggest that the first major subaerial land-building event of New Guinea occurred between 35 and 30 Mya with the subduction of the Australian continent beneath an Inner Melanesian Arc, uplifting and exposing the Papuan Peninsula (south-eastern peninsula in modern day New Guinea—EPCT). A later cascading orogeny proceeding west (15 Mya) to east (3 Mya) gave rise to the Central Cordillera at its present elevation roughly 5 Mya. Under this scenario, the earliest New Guinean terrestrial fauna (Oligocene) to diversify in New Guinea are expected to show early colonization of the EPCT due to it being the first available subaerial landmass until the Mid-Miocene (~10 Mya), with subsequent dispersal through an actively uplifting Fold Belt (Toussaint *et al.* 2014).

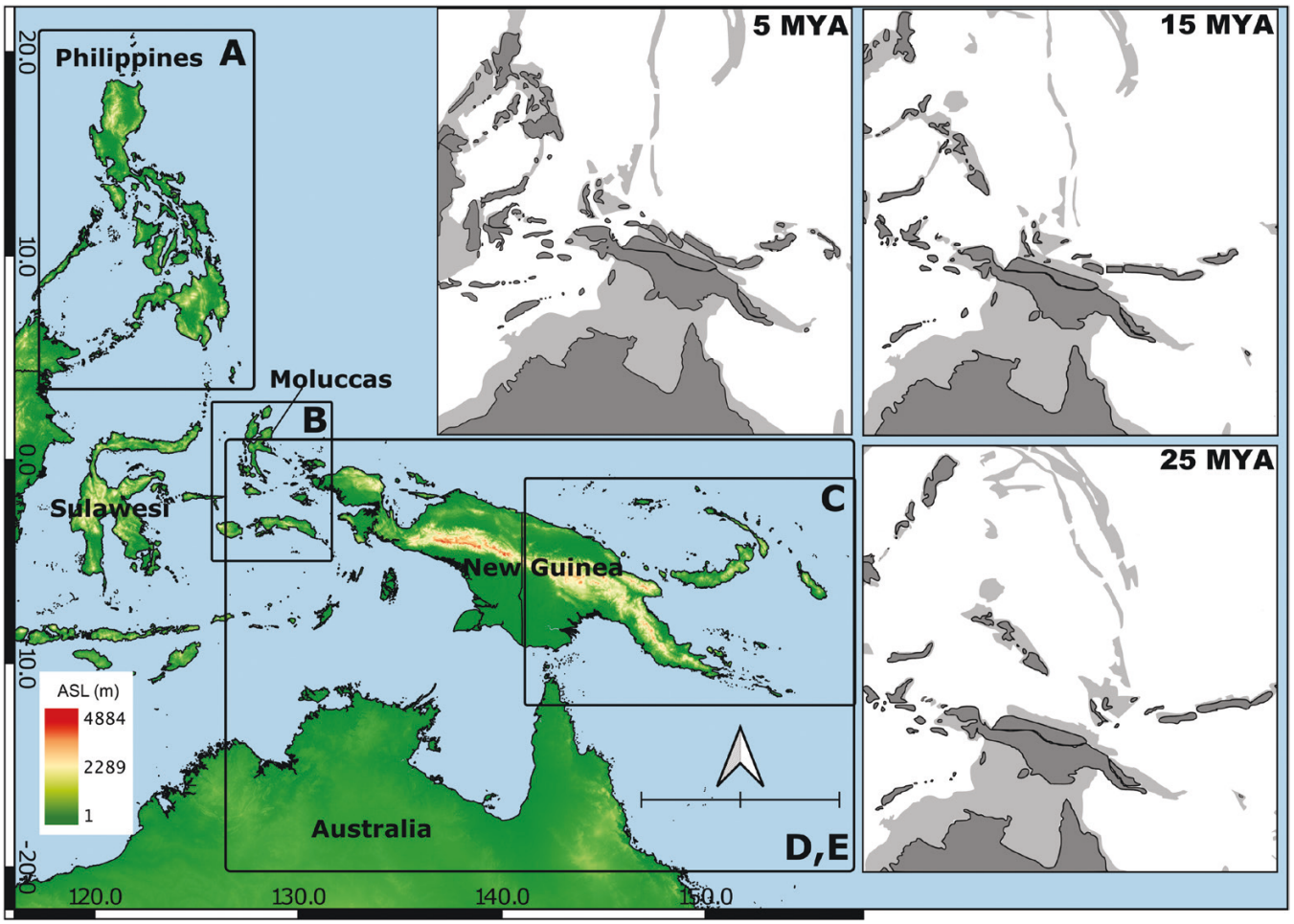

Figure 1. Map of the western Pacific Islands that comprise the current geographic range of *Tropidonophis*. Black boxes and callout letters refer to the expanded maps in Figure 2, and the scale bar represents 1000 km. The three caption boxes are schematics of the Pacific and its island positions through the Miocene to present day, adapted from Hall (2002) published in *J. of Asian Earth Sciences*. The light grey shading represents extensions of landmasses that were subaerial during time periods of low sea level.

Sunda-Papuan keelbacks (Natricidae: *Tropidonophis* Jan 1863) are a group of 20 semi-aquatic snake species distributed in the Philippines (three species), south-eastward into the Moluccas (four species), and eastward into New Guinea (and adjacent archipelagos, 13 species) and Australia (one species shared with New Guinea) (Figs 1, 2; Malnate and Underwood 1988, Deepak *et al.* 2021). Other Pacific colubroid snake lineages exhibit similar biogeographical trends: cat-eyed snakes (Colubridae: *Boiga* Fitzinger 1826), bronzeback snakes (Colubridae: *Dendrelaphis* Boulenger 1890), and groundsnakes (Colubridae: *Stegonotus* Duméril 1854). However, Sunda-Papuan keelbacks are the only natricid lineage to disperse east of Lydekker's Line into New Guinea and Australia, providing an additional phylogenetic contrast to examine colubroid biogeography and diversification in New Guinea. Malnate and Underwood (1988) provided a complete treatment of this group, with elevation of *Tropidonophis* Jan 1863 to genus level, assignment of 14 species to the genus, descriptions of four new species, and inference of the first phylogeny and hypothesis of historical biogeography based on a dataset of 34 morphological characters. Malnate and Underwood's (1988) hypothesis for *Tropidonophis* biogeography had five major components: (i) the most recent common ancestor (MRCA) of *Tropidonophis* diverged from a South-East Asian ancestor and dispersed across the Sunda Shelf into the Philippine Islands, (ii) the genus continued dispersal eastward to the Moluccas, (iii) the Bismarck Archipelago was reached prior to mainland New Guinea via a northern arc of islands distinct from the New Guinea mainland, (iv) colonization of New Guinea from the Moluccan taxa probably occurred more than once, and, lastly, (v) *Tropidonophis* species on New Guinea are monophyletic. Only three works since Malnate and Underwood (1988) have examined *Tropidonophis* within a systematic or evolutionary context: Kraus and Allison (2004) described a new species from the D'Entrecasteaux Archipelago in New Guinea (*Tropidonophis dolasii* Kraus and Allison 2004); Zaher *et al.* (2019) included one species from

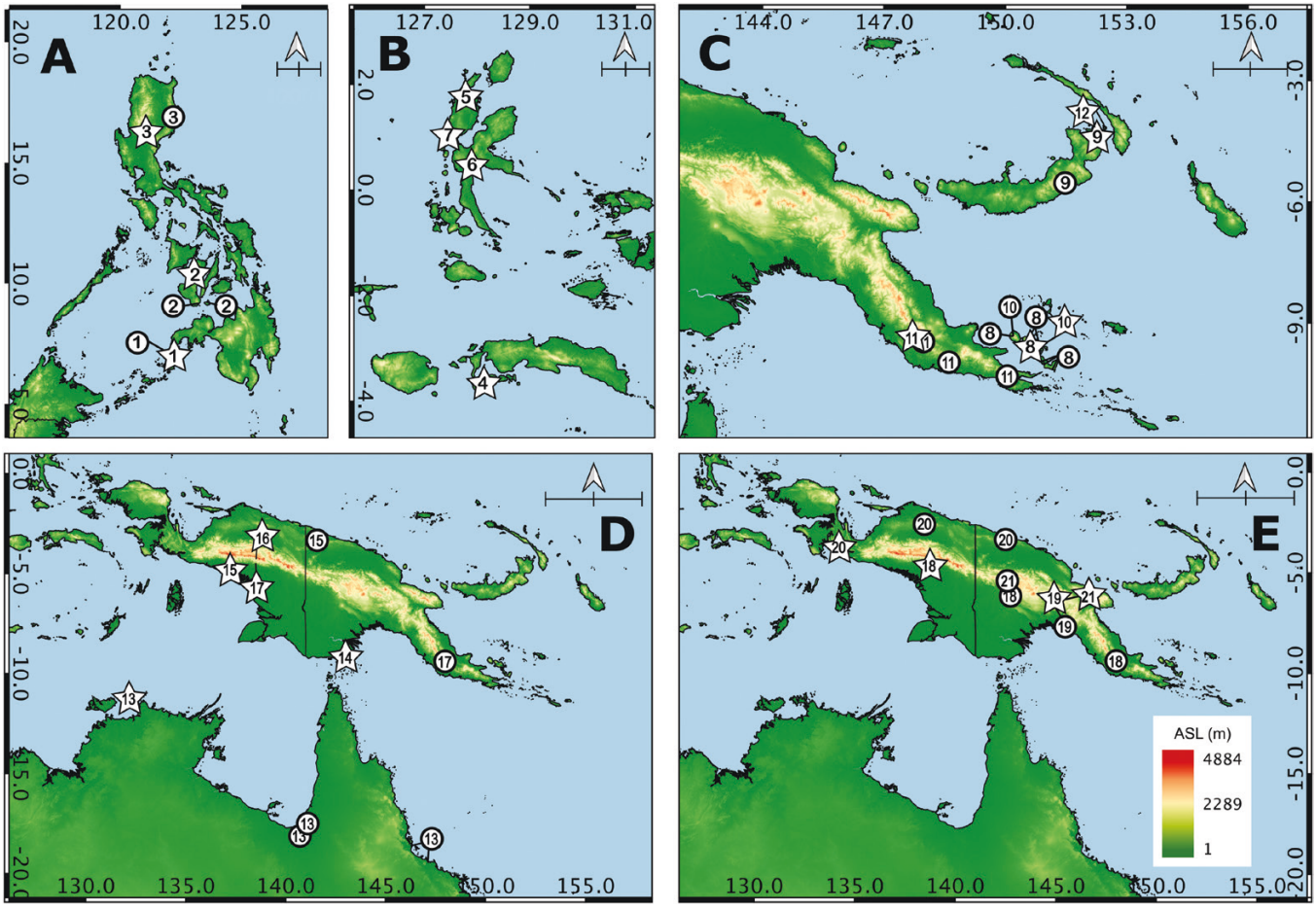

Figure 2. Expanded maps of the Pacific Islands that comprise the distribution of species of *Tropidonophis*. White circles indicate location of specimens included in our phylogenetic analyses; stars indicate type localities. Species only represented by star symbols are taxa not included in our analyses. A, map of the Philippines showing localities for (1) *Tr. dendrophiops*, (2) *Tr. negrosensis*, and (3) *Tr. spilogaster*; scale bar represents 200 km. B, map of the Molucca Islands showing the type localities of (4) *Tr. elongatus*, (5) *Tr. halmahericus*, (6) *Tr. punctiventris*, and (7) *Tr. truncatus*; scale bar represents 100 km. C, map of New Guinea and northern Australia showing sampling and type localities for (8) *Tr. aenigmaticus*, (9) *Tr. dahlii*, (10) *Tr. dolasii*, (11) *Tr. doriae*, and (12) *Tr. hypomelas*; scale bar represents 200 km. D, map of New Guinea and northern Australia showing sampling and type localities for (13) *Tr. mairii mairii*, (14) *Tr. mairii plumbea*, (15) *Tr. mcdowelli*, (16) *Tr. montanus*, and (17) *Tr. multiscutellaus*; scale bar represents 500 km. E, map of New Guinea and northern Australia showing sampling and type localities (18) *Tr. novaeguineae*, (19) *Tr. parkeri*, (20) *Tr. picturatus*, and (21) *Tr. statisticus*; scale bar represents 500 km.

the Philippines, *Tropidonophis dendrophiops* (Günther 1883), in a 15 locus (six mitochondrial, nine nuclear) phylogeny of all snakes; and Deepak *et al.* (2021) performed a family-wide phylogenetic analysis of Natricidae, including the first DNA sequence-based phylogeny of multiple *Tropidonophis* spp. (11 species; three mitochondrial and four nuclear loci). Deepak *et al.* (2021) found a paraphyletic *Tropidonophis sensu* Malnate and Underwood (1988), and reassigned the Philippine taxon, *Rhabdophis spilogaster* (Boie 1827), to render the latter monophyletic. The scope of this work was broad, examining natricids for biogeographic and macroevolutionary patterns and did not provide detailed comparisons of trees and biogeography with those of Malnate and Underwood (1988). Here, we provide the most-inclusive phylogenetic estimations for *Tropidonophis* based on nearly 3000 nuclear genomic loci. We infer robust hypotheses of systematics and biogeography of the Sunda-Papuan keelbacks to test the biogeographic and systematic hypotheses presented by Malnate and Underwood (1988).

MATERIALS AND METHODS

DNA extraction, genomic sequencing, ultraconserved elements' bioinformatics

We extracted DNA using either a salt-extraction protocol (Austin *et al.* 2010) or Qiagen DNEasy Blood and Tissue Kits for 44 samples [Australian Biological Tissue Collection (ABTC), Bernice P. Bishop Museum (BPBM), and Louisiana State University Museum of Natural Sciences (LSUMZ) samples, Table 1]. Samples received on loan from The University of Kansas Natural History Museum were received as loans of DNA extracts, not ethanol tissue subsamples. Library preparation for ultraconserved elements (UCEs) targeted-sequence capture followed the protocol described in Faircloth *et al.* (2012). UCE sequencing was performed in two separate instalments: first through the sequencing facilities at the Duke University Center for Genomic and Computational Biology (Durham, North Carolina, USA) and then through Daicel Arbor Biosciences (Ann Arbor, Michigan, USA). All libraries were dual indexed with iTru primers (Glenn *et al.* 2019). UCEs were obtained from raw read data by following the *phyluce 1.6* pipeline (Faircloth 2016). Raw reads were trimmed and cleaned using *illumiprocessor* (Faircloth 2013) and *trimmomatic* (Del Fabbro *et al.* 2013, Bolger *et al.* 2014), both implemented within *phyluce*. The split-adapter-quality-trimmed raw reads were then used as input for UCE assembly. Many options are available within *phyluce* for UCE assembly, but we deviated from the traditional pipeline and used *itero* (Faircloth 2018), a guided assembler that integrates spades (Prjibelski *et al.* 2020), bwa (Li and Durbin 2009), and samtools (Danecek *et al.* 2021) to produce assembled contigs from a targeted probe set, in this case the Tetrapods 5K UCE Probeset. Samples were split into five-sample batches to prevent premature termination due to computational walltime. All assembly runs were performed on the Louisiana State University High Performance Computing resources. Final assembly statistics can be found in Table 1. After successful assembly, samples were returned to the traditional *phyluce* pipeline, creating an SQL database with the *phyluce_assembly_match_contigs* command. After SQL database creation, we performed *phyluce_assembly_get_match_counts* to create our data matrix configuration file. Matrix creation permits easy retrieval of individual UCE FASTAs using *phyluce_assembly_get_fastas_from_match_counts*, which facilitates organization of new dataset combinations. We then performed joint UCE alignment through MAFFT (Katoh and Standley 2013) and edge-trimming with *phyluce_align_seqcap_align*. Internal trimming was not performed due to the medium-to-shallow divergence (<50 Mya) of our ingroup (Faircloth *et al.* 2012). Individually aligned UCEs were then concatenated and formatted for phylogenetic analyses under maximum likelihood and Bayesian frameworks. All cleaned raw UCE reads and input files for downstream analyses have been deposited in Dryad (DOI: 10.5061/dryad.zw3r228f9).

Concatenated analyses

For the concatenated phylogenetic analyses, we created an incomplete UCE matrix that permits alignment concatenation based on percent inclusion of samples per locus. For phylogenetic inference within a maximum-likelihood framework, we chose RAxML v.8.2.12 (Stamatakis 2014) with the GTRGAMMA model. RAxML was executed in three steps for tree inference. We first performed 20 searches for the best tree under ML. We then generated bootstrap data using the autoMRE function, which converged after 100 bootstrap replicates. Lastly, we reconciled the best tree with the bootstrap replicates to provide our final bootstrapped tree (Fig. 3). In addition to maximum likelihood, we analysed our concatenated alignment within a Bayesian framework. For this, we used ExaBayes v.1.5 (Aberer, Kobert and Stamatakis 2014) with the GTRGAMMA model. ExaBayes was executed for 2 million generations to sample four independent runs of four Markov chains, with posterior-guided subtree pruning and regrafting (likeSpr) = 4, parsimony-biased subtree pruning and regrafting (parsimonySPR) = 8, stochastic nearest neighbour interchange (stNNI) = 4, extending subtree pruning and regrafting (eSPR) = 4, Newton–Raphson-based branch length proposal employing a Gamma distribution (blDistGamma) = 7, and multiplier on branch lengths (branchMulti) = 2. Together with implementation of Metropolis-coupling, these parameter modifications have been shown to ensure proper mixing and aid in sampling tree space, especially with difficult datasets (Blair *et al.* 2019). Sumtrees within DendroPy v.4.5.2 (Sukumaran and Holder 2010) was used to generate a consensus tree from the four independent tree runs discarding the first 10% of samples of the posterior as burn-in, and TRACER v.1.7.1 (Rambaut *et al.* 2018) was used to view four parameter outputs from each run and to check for convergence among all four runs. Our concatenated analyses were run through the Louisiana State University High Performance Computing for the RAxML analyses and the CIPRES Science Gateway (Miller *et al.* 2011) for the ExaBayes analyses.

Coalescent species-tree analyses

Coalescent-based methods that require individual UCE gene trees as input have a tendency to provide trees with lower support and resolution compared to quartet-based analyses, which consider the entirety of the concatenated UCE alignment while inferring species-trees within a multi-species coalescent

Table 1. Represented taxa in UCE phylogenies.

Genus	Species	Catalogue No.	Field No.	Country	Province	Paired Reads	No. UCEs	Latitude	Longitude
Opisthotropis	*alcalai*	KU 334751	n/a	Philippines	Zamboanga C.	3 062 533	2533	7.0711	122.0755
Opisthotropis	*typicus*	KU 327424	n/a	Philippines	Palawan	2 219 674	3011	8.908132	117.767161
Rhabdophis	*lineatus*	KU 321764	RMB 11182	Philippines	Zamboanga C.	3 635 278	2554	7.0711	122.0755
Rhabdophis	*lineatus*	KU 334923	RMB 17393	Philippines	Zamboanga C.	3 006 797	2795	7.0711	122.0755
Rhabdophis	*subminiatus*	KU 311557	KU-FS 304	China	Guangxi	3 699 856	2648	21.89264	107.82824
Thamnophis	*sirtalis*	UTA R-62823	EDBJR-23777	US	Oregon	n/a	3073	44.699172	−123.221683
Tropidonophis	*aenigmaticus*	BPBM 16535	FK 6266	PNG	Milne Bay	1 537 609	3118	−9.45199	150.825
Tropidonophis	*aenigmaticus*	BPBM 16536	FK 6405	PNG	Milne Bay	1 606 661	3099	−9.45617	150.56
Tropidonophis	*aenigmaticus*	BPBM 16537	FK 6622	PNG	Milne Bay	1 614 792	3088	−9.96373	150.955
Tropidonophis	*aenigmaticus*	BPBM 17242	FK 7185	PNG	Milne Bay	1 840 477	3015	−10.034	150.982
Tropidonophis	*aenigmaticus*	BPBM 17243	FK 7281	PNG	Milne Bay	1 152 653	3231	−10.1358	150.971
Tropidonophis	*aenigmaticus*	LSUMZ 98047	CCA 15606	PNG	Milne Bay	1 133 250	2787	−9.2650667	150.223883
Tropidonophis	*dahlii*	BPBM 22555	FK 11003	PNG	E. New Britain	11 315 124	2215	−5.51902	151.502
Tropidonophis	*dahlii*	BPBM 22558	FK 11107	PNG	E. New Britain	2 314 597	3105	−5.51902	151.502
Tropidonophis	*dendrophiops*	KU 314999	RMB 10362	Philippines	Zamboanga C.	5 257 023	1969	6.952623	122.074763
Tropidonophis	*dendrophiops*	KU 321698	RMB 11596	Philippines	Zamboanga C.	4 369 512	2148	6.952623	122.074763
Tropidonophis	*dolasii*	BPBM 16539	FK 6118	PNG	Milne Bay	5 557 419	2991	−9.4555	150.786
Tropidonophis	*dolasii*	LSUMZ 98044	CCA 15457	PNG	Milne Bay	2 627 793	1984	−9.2888833	150.2145
Tropidonophis	*dolasii*	LSUMZ 98045	CCA 15473	PNG	Milne Bay	4 008 587	3091	−9.2899667	150.21425
Tropidonophis	*doriae*	BPBM 19485	FK 8852	PNG	Central	1 640 201	3255	−9.44387	147.984
Tropidonophis	*doriae*	BPBM 19486	FK 8860	PNG	Central	1 913 210	3240	−9.44387	147.984
Tropidonophis	*doriae*	LSUMZ 129280	CCA 17748	PNG	Central	3 374 847	2944	−9.442142	147.98516
Tropidonophis	*doriae*	LSUMZ 96086	CCA 4676	PNG	Milne Bay	1 652 896	2916	−10.325617	150.03765
Tropidonophis	*doriae*	LSUMZ 96087	CCA 5698	PNG	Central	2 271 894	2048	−9.9824	148.578517
Tropidonophis	*mairii*	ABTC 102464	n/a	Australia	Queensland	3 879 107	2276	−17.726111	141.01
Tropidonophis	*mairii*	ABTC 72853	n/a	Australia	Queensland	3 770 330	2983	−17.925	140.7
Tropidonophis	*mairii*	ABTC 83021	n/a	Australia	Queensland	5 845 852	2176	−19.375	147.0631
Tropidonophis	*mairii*	ABTC 83046	n/a	Australia	Queensland	3 260 445	2647	−18.6108	146.1781
Tropidonophis	*mcdowelli*	LSUMZ 96092	CCA 2957	PNG	Sandaun	691 229	3139	−3.3960833	141.5829
Tropidonophis	*multiscutellatus*	BPBM 19487	FK 8735	PNG	Central	1 666 867	3148	−9.46252	147.922
Tropidonophis	*multiscutellatus*	BPBM 19488	FK 8758	PNG	Central	1 117 871	3328	−9.44387	147.984
Tropidonophis	*multiscutellatus*	BPBM 19489	FK 8800	PNG	Central	668 180	3384	−9.44387	147.984
Tropidonophis	*multiscutellatus*	BPBM 19490	FK 8801	PNG	Central	1 851 693	3166	−9.44387	147.984
Tropidonophis	*multiscutellatus*	BPBM 19491	FK 8809	PNG	Central	960 469	3162	−9.44387	147.984
Tropidonophis	*multiscutellatus*	BPBM 19492	FK 8837	PNG	Central	588 384	3435	−9.44387	147.984
Tropidonophis	*multiscutellatus*	BPBM 19494	FK 9257	PNG	Central	1 731 161	3338	−9.44387	147.984

Table 1. Continued

Genus	Species	Catalogue No.	Field No.	Country	Province	Paired Reads	No. UCEs	Latitude	Longitude
Tropidonophis	*multiscutellatus*	LSUMZ 129274	CCA 17751	PNG	Central	5 199 245	2833	–9.442142	147.98516
Tropidonophis	*multiscutellatus*	LSUMZ 129286	CCA 17726	PNG	Central	5 078 282	2794	–9.442142	147.98516
Tropidonophis	*multiscutellatus*	LSUMZ 129287	CCA 17738	PNG	Central	5 070 199	2828	–9.442142	147.98516
Tropidonophis	*multiscutellatus*	LSUMZ 98519	CCA 17054	PNG	Milne Bay	622 714	2957	–9.4421667	147.98555
Tropidonophis	*negrosensis*	KU 303026	CDS 947	Philippines	Negros Oriental	2 953 756	2569	9.243382	123.177822
Tropidonophis	*negrosensis*	KU 331736	RMB 15244	Philippines	Siquijor	5 741 486	2667	9.191437	123.584788
Tropidonophis	*novaeguineae*	ABTC 45572	n/a	PNG	Hela	3 585 012	2862	–6.2	142.766
Tropidonophis	*novaeguineae*	LSUMZ 129271	CCA 17749	PNG	Central	4 545 980	2855	–9.444183	147.999521
Tropidonophis	*parkeri*	ABTC 43185	n/a	PNG	Chimbu	4 324 705	2464	–6.533333	144.85
Tropidonophis	*picturatus*	ABTC 90275	n/a	Indonesia	Papua	4 078 947	2779	–2.59755	138.446833
Tropidonophis	*picturatus*	BPBM 23454	FK 11480	PNG	West Sepik	1 223 728	3333	–3.42457	142.519
Tropidonophis	*spilogaster*	KU 327287	ACD 1758	Philippines	Isabela	4 950 541	2680	16.961751	122.032783
Tropidonophis	*spilogaster*	KU 327293	ACD 2829	Philippines	Isabela	4 872 286	2427	16.961751	122.032783
Tropidonophis	*statisticus*	BPBM 34389	FK 12825	PNG	Southern H.	1 259 574	3085	–5.6431	142.6342
Tropidonophis	*statisticus*	BPBM 34393	FK 13134	PNG	Southern H.	2 568 573	2806	–5.6456	142.65052
Tropidonophis	*statisticus*	BPBM 34394	FK 13135	PNG	Southern H.	2 563 343	3149	–5.64545	142.63904
Tropidonophis	*statisticus*	BPBM 34395	FK 13136	PNG	Southern H.	1 324 882	3336	–5.6431	142.6342
Tropidonophis	*statisticus*	BPBM 34398	FK 13183	PNG	Southern H.	2 146 532	3209	–5.65479	142.64997
Tropidonophis	*statisticus*	BPBM 34399	FK 13184	PNG	Southern H.	1 937 227	3317	–5.65479	142.64997
Tropidonophis	*statisticus*	BPBM 34400	FK 13186	PNG	Southern H.	1 020 115	3350	–5.64545	142.63904
Xenochrophis	*trianguligerus*	KU 328567	DSM 926	Thailand	N. Si Thammarat	3 228 734	2383	8.492948	99.729656

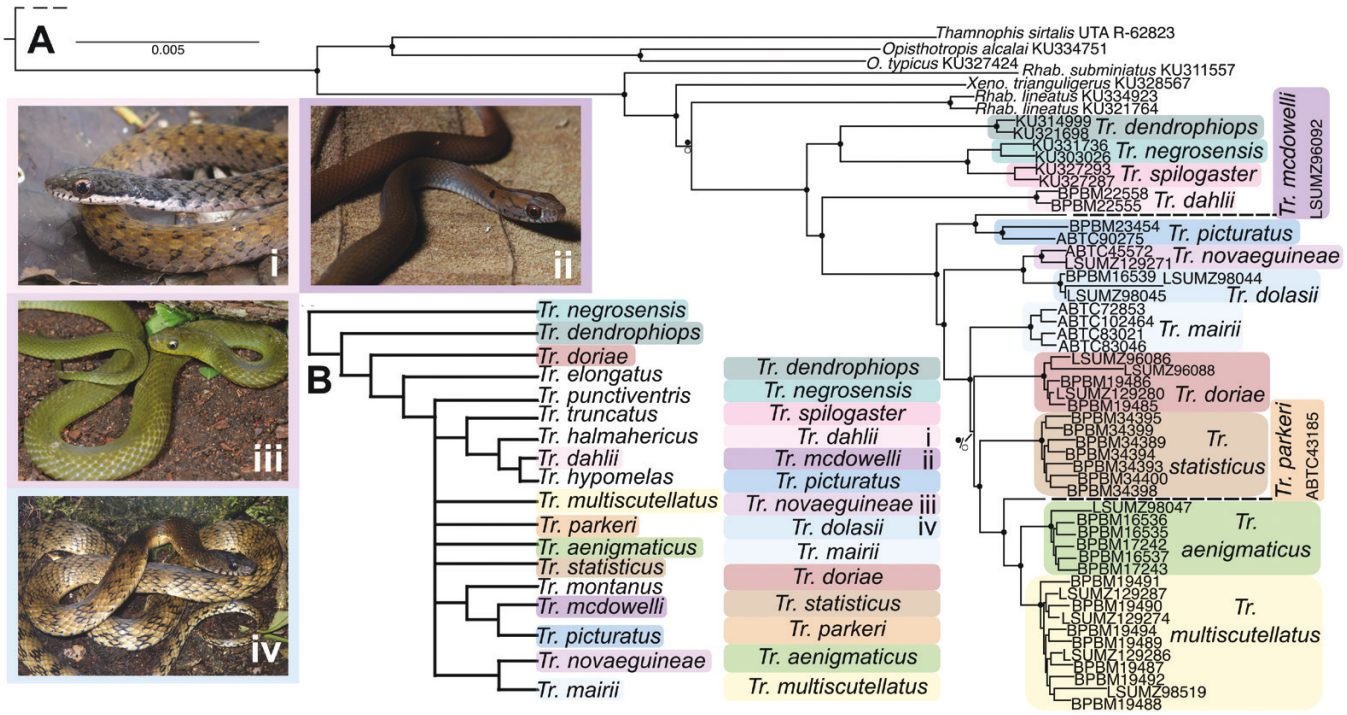

Figure 3. A, concatenated 75% completion UCE phylogeny comprising 2059 loci from RAxML. Nodal supports are represented by circles on the node (black circle: bootstrap = 100, posterior probability = 1; white circle: 80 < bootstrap < 100, 0.80 < posterior probability < 1.00). A single black circle at the node indicates a bootstrap = 100 and posterior probability = 1.00, and two circles indicate node posterior probability (top circle) and node bootstrap support (bottom circle). To maintain tree clarity, intraspecific nodal support values have not been included. Field photos are of specimens represented in the phylogeny. Photos are *Tr. dahlii* BPBM 22558 (i), *Tr. mcdowelli* LSUMZ 96092 (ii), *Tr. novaeguineae* LSUMZ 129271 (iii), and *Tr. dolasii* LSUMZ 98045 (iv). B, morphology-based dendrogram inferred in Malnate and Underwood (1988).

framework (Mirarab *et al.* 2014, Roch and Warnow 2015, Zhang *et al.* 2018, Salter *et al.* 2020, Wascher and Kubatko 2021). For this reason, we used SVDQuartets (Chifman and Kubatko 2014) within PAUP* 4.0a161 (Swofford 2003) for the coalescent-based analysis. We first assigned each sample ($N = 61$) a priori to our species' identifications and ran our 'tip-assigned' analysis using exhaustive quartet sampling (349 506 quartets) with 100 bootstrap replicates. This analysis was duplicated for a 'tip-unassigned' analysis, which included all samples but with no a priori species assignment (521 855 quartets), thus treating each tip as potentially an independently evolving lineage. Consensus trees from each analysis were printed in nexus format using the *saveTrees* command in PAUP. Because SVDQuartets will accept entire concatenated alignments as input, we also used a second species-tree method that satisfied the coalescent using a more traditional gene-tree coalescent procedure. For this method, we used the StarBEAST2 package (Ogilvie *et al.* 2017) implemented in BEAST v.2.6.6 (Bouckaert *et al.* 2019). For our StarBEAST analysis, we first filtered and selected our 50 most phylogenetic informative UCE loci using the *phyluce_align_get_informative_sites* command within *phyluce*. We selected the 50 most informative UCE loci from a 95% taxa completion matrix, versus the 75% inclusivity matrix used for the concatenated analyses. We chose 50 loci since Ogilvie *et al.* (2017) used a simulated dataset of 52 loci for their description of StarBEAST2 when showing effectiveness based on loci number. Second, other studies have shown success using this same method with only 32 loci (Reynolds *et al.* 2022) and even as low as eight UCEs (Campbell *et al.* 2020). We included all samples (Table 1) as we did with concatenated analyses above, but we assigned each tip species identification prior to executing inferences. We linked clock models for all 50 loci, and we ran inferences under a strict clock model with the StarBEAST option to estimate rates. Each site model was identical, but not linked, for all 50 loci (HKY, estimated base frequencies). Due to the large number of loci for a BEAST analysis, HKY with estimated base frequencies provides a more realistic substitution model than Jukes Cantor, but also greatly reduces computational burden than other more complex models (Hasegawa *et al.* 1985, Ogilvie *et al.* 2017). Gene ploidy was set to 2.0 for all loci. For population modelling within StarBEAST, we selected the Analytical Population Size Integration option to again optimize computation time. We used a birth–death model prior, allowing estimation of birth and death rates. We ran two identical StarBEAST runs independently of each other for 200 million generations. Convergence of these runs was checked and confirmed in TRACER v1.7.1. We performed a 50% burn-in and combined the logs and tree outputs for these two runs in LogCombiner within BEAST v.2.6.6 (Bouckaert *et al.* 2019) before generating a consensus tree in Sumtrees.

Divergence dating

We used two approaches to construct the first time-calibrated phylogenies for this group: a penalized likelihood approach through treePL based on our concatenated tree inference

(Smith and O'Meara 2012) and joint divergence dating with species-tree inference with StarBEAST based on our 50 most-informative UCE loci within our 95% completion matrix. treePL is a commonly used divergence-dating program that uses penalized likelihood with any input tree to produce an ultrametric chronogram tree with estimated node ages. StarBEAST provides divergence dating within a Bayesian framework and conducts joint species-tree inference through coalescence-based gene-tree estimation. For both dating methods, we used the Natricidae crown mean age and 95% confidence interval found in the most recent dated estimate of all Squamata based on reduced representation datasets and extensive squamate fossil calibrations (Burbrink *et al.* 2019; see Burbrink *et al.*'s supplemental tree S9). Under a log-normal distribution, the mean (M) date and standard deviation (SD) used were—Natricidae: M = 27.6, SD = 0.035. treePL does not allow mean and standard-deviation data for date calibrations; rather it takes a minimum and maximum age range; thus, we used the upper and lower bounds of the Natricidae 95% confidence interval for our treePL analyses (29.2–26.0 Mya). However, Deepak *et al.* (2021) inferred an older date for the Natricidae crown due to the inclusion of the earliest branching natricid *Amphiesmoides ornaticeps* in their inferences, a species never before represented in sequence-based phylogenies. They inferred the Natricidae age to be 39.0 Mya using treePL. For this reason, we also ran treePL using the Deepak *et al.* (2021) Natricidae crown age as a secondary node calibration. Previous workers have treated this clade of snakes as the subfamily Natricinae within a large Colubridae (Zaher *et al.* 2019, Deepak *et al.* 2021). Here, we use the taxonomy and systematics presented in Burbrink *et al.* (2019), referring to this clade as the family Natricidae. Divergence dates inferred by treePL are reported as point estimates without a confidence interval, and dates inferred by StarBEAST are reported as the mean divergence date with the 95% confidence interval in parentheses immediately following the mean.

We used our RAxML tree topology (Fig. 3) as input for all treePL inferences. Prior to treePL, we rooted the tree with our outgroup (*Stegonotus* + *Lycodon*) in the R package *ape* (Paradis *et al.* 2004). treePL was implemented using a three-step procedure recommended in the documentation. First, we used the *prime* function within the configuration file to find the most appropriate parameters for penalized likelihood analysis. Second, we used cross-validation (*cv* function) to search for the best smoothing parameter. Lastly, using the results of both *prime* and *cv*, we performed the *smooth* function based on the preferred chi-squared setting. The output was our RAxML topology converted to an ultrametric tree with dated nodes. All output chronograms were then processed with a personalized R script (JRR) to plot the trees along the current accepted geologic timetable (Gradstein, Ogg and Hilgen 2012), as well as the 95% confidence intervals (StarBEAST) on each node. This script utilized *geoscalePhylo* within *strap* v.1.6-0 (Bell and Lloyd 2015) and confidence interval scripts within R (Černy 2020).

Ancestral biogeography

We used the program Reconstruct Ancestral State in Phylogenies (RASP4; Yu *et al.* 2020) to estimate historical biogeography. We used our treePL and StarBEAST output chronograms as input consensus trees to infer ancestral biogeography within *Tropidonophis* in two separate analyses. RASP4 provides a useful interface for performing ancestral biogeographic analyses because it runs BioGeoBEARS (Matzke 2014) within the interface. Prior to both model test and reconstruction, we used RASP4 to prune the input trees to include only one tip per species, and to remove our non-natricid outgroups, as well as deeply divergent representative natricids (*Thamnophis sirtalis* and *Opisthotropis* spp.). We performed BioGeoBEARs model test within RASP. The most appropriate model was chosen based on weighted AICc, as recommended by BioGeoBEARS. The +J parameter and its bias during model testing has been reviewed and debated extensively (Ree and Sanmartin 2018). However, most recently, the +J parameter was re-evaluated using DEC vs. DEC+J and was shown to be a valid parameter in ModelTest (Matzke 2022). Because the organisms in this study are island animals that are suspected to have dispersed by rafting on vegetation mats and other founder events, we included +J in model test due to the biological relevance of this model parameter (Deepak *et al.* 2021). Lastly, we performed model testing and subsequent reconstructions on each of our two dated trees: treePL-dated (concatenated UCEs, 75% completion) and StarBEAST tree (50 most-informative-UCEs, 95% completion).

We assigned range estimates for the Philippine taxa [*R. lineatus* (Peters 1861), *Tr. spilogaster*, *Tr. dendrophiops*, *Tr. negrosensis* (Taylor, 1917)] on Leviton *et al.* (2018). Based on confirmed specimen records, we assigned each Philippine species to one of the Pleistocene Aggregate Island Complexes of the Philippines (hereafter PAIC; Brown and Diesmos 2009). We based New Guinean *Tropidonophis* range assignments on the geographic sampling in this study. We did not adhere to the ranges reported in the most current revision of this genus (Malnate and Underwood 1988), because they are too broad. Based on ongoing integrative data collection, both morphological (scalation patterns, scale counts, μCT scanning) and molecular, many species *sensu* Malnate and Underwood (1988) contain taxa that have yet to be described and are not represented in this study. For this reason, when possible, the taxa included are represented by either typic or topotypic sampling and have been further confirmed by specimen examination (JRR). *Tropidonophis* species in this tree that are not represented by topotypic samples are *Tropidonophis mcdowelli* Malnate and Underwood 1988, *Tropidonophis multiscutellatus* (Brongersma 1948), *Tropidonophis novaeguineae* (Lidth de Jeude 1911), and *Tropidonophis picturatus* (Schlegel 1837). We were unable to obtain genetic material of these species from the vicinities of their type localities (see Fig. 2).

RESULTS

Sequencing and concatenated analyses

UCE sequencing results can be seen in Table 1. Our paired-end read counts were based on the cleaning statistics from *illumiprocessor* and do not include un-paired reads. Our mean paired reads were 2 948 931, with a mean UCE recovery of 2872 (Table 1) across our 61 samples. We created a 75% taxa completion matrix that comprised 2059 aligned and concatenated UCEs from our targeted sequence capture. Our

maximum-likelihood and Bayesian analyses produced identical topologies with strong support (all 1/100 posterior probability and bootstrap) for all 14 *Tropidonophis* species identified a priori (Fig. 3). Our concatenated phylogenies mostly corroborate the phylogeny in Deepak *et al.* (2021). The Philippine species *Rhabdophis lineatus* and *R. spilogaster* were also found in similar paraphyletic phylogenetic positions supporting the taxonomic hypothesis that *Tropidonophis sensu* Malnate and Underwood (1988) is paraphyletic. *Rhabdophis spilogaster* is found sister to *Tr. negrosensis*, supporting the taxonomic reassignment of *R. spilogaster* to *Tropidonophis sensu* Deepak *et al.* (2021). Philippine *Tropidonophis* species (*Tr. dendrophiops*, *Tr. negrosensis*, and *Tr. spilogaster*) are monophyletic and strongly supported as sister to a monophyletic New Guinean *Tropidonophis* (100 bootstrap; 1.00 PP).

Species-tree inference

The StarBEAST analysis (Fig. 4A) found strong support for all species' identifications made a priori. As in our concatenated analyses, *Tropidonophis sensu* Deepak *et al.* (2021) was monophyletic, with reciprocally monophyletic Philippine and New Guinean clades (Fig. 4A). Our StarBEAST inferences within *Tropidonophis* are also completely congruent with the ML and Bayesian concatenated analyses (Fig. 3), with the only discordance existing in the relationship between outgroup taxa [*R. lineatus* and *Xenochrophis trianguligerus* (Boie 1827)]. Within SVDQuartets we ran two separate analyses comprising a 'tip-unassigned' and a 'tip-assigned' inference. The trees were identical in topology and nearly identical in bootstrap support (Figs 4B, 5B). Only two nodes showed low support (<75 bootstrap) in our 'tip-assigned' SVDQuartet inference: (i) the clade including *R. lineatus* and all *Tropidonophis* species (bootstrap = 67) and (ii) the *Tropidonophis mairii* (Gray 1841) and *Tropidonophis doriae* (Boulenger 1898) clade (49). Within our 'tip-unassigned' SVDquartet inference, these nodes were found with 74 and 48 bootstrap values, respectively. The low support for *R. lineatus* + *Tropidonophis* spp. is probably due to extensive paraphyly within *Rhabdophis* (Rafe Brown, unpublished data) and our sparse representation of other *Rhabdophis* species given that our focus was *Tropidonophis*. All *Tropidonophis* species were found reciprocally monophyletic in both the 'tip-unassigned' SVDQuartets' (Fig. 5B) tree and our UCE concatenated phylogeny (Fig. 3), providing strong evidence that our a priori species' identifications were correct for included samples. In addition, and most relevant for the focus of this work, both species' tree inferences found a monophyletic *Tropidonophis*, with a monophyletic Philippine clade sister to a monophyletic New Guinea clade that corroborate the concatenated analyses (Fig. 3). Comparing our SVDQuartets' 'tip-assigned' inference to our StarBEAST tree (Fig. 4), the two phylogenies were strongly congruent, with just a few inconsistencies. First, outside of *Tropidonophis*, StarBEAST (Fig. 4A) found *R. lineatus* and *X. trianguligerus* to be sister to each other, while SVDQuartets found *X. trianguligerus* sister to a *R. lineatus* and all *Tropidonophis* clade (Fig. 4B). Another difference relates to the relationship between *Tr. mairii* and *Tr. doriae*. The StarBEAST tree found the same topology as our concatenated

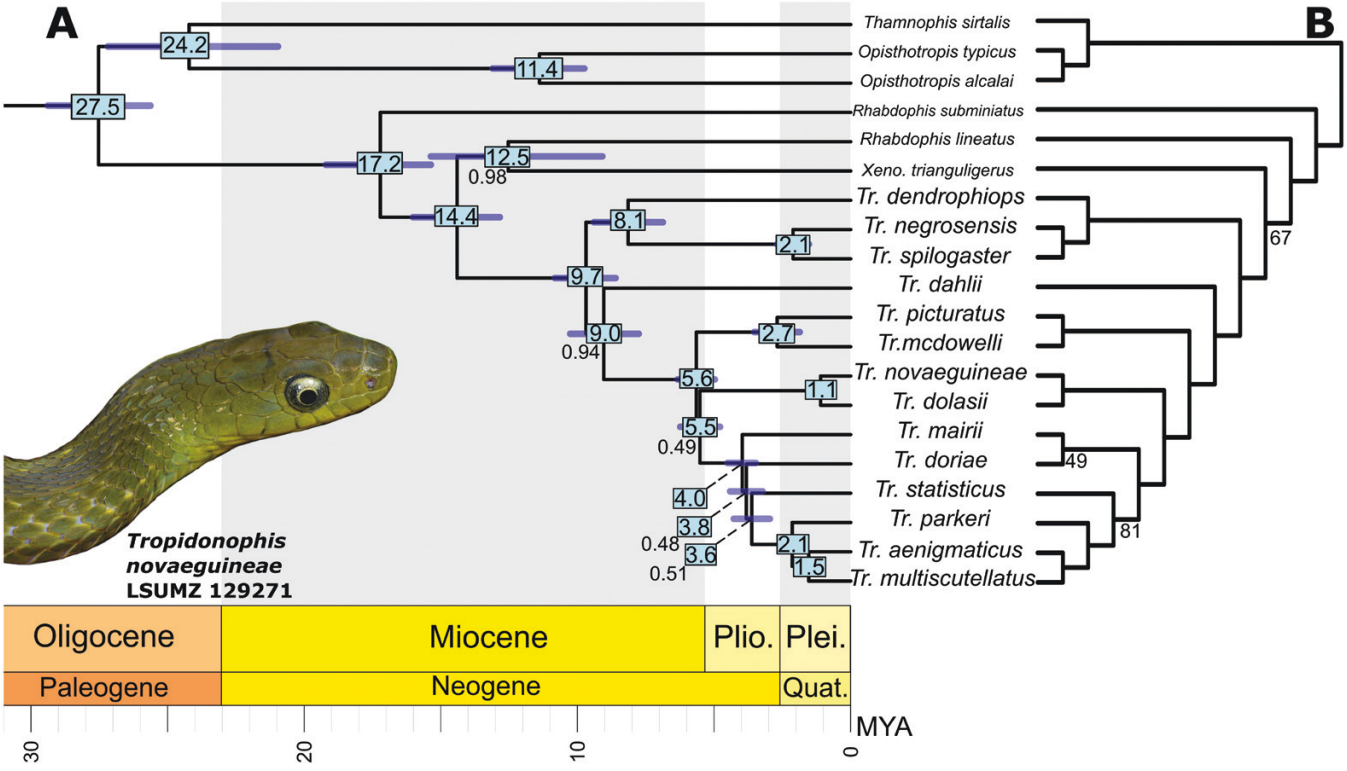

Figure 4. Species-tree estimations based on: A, StarBEAST2; B, SVDQuartets. All node support values are either (A) 1.00 posterior probability or (B) 100 bootstrap, unless otherwise noted. The nodal bars represent the 95% confidence interval for mean divergence date, with the distribution mean displayed to one decimal place in 1 million years on the node. The X-axis represents time in million years; Plio. = Pliocene, Plei. = Pleistocene, Quat. = Quaternary.

analyses, with *Tr. mairii* sister to a clade containing *Tr. doriae* and other New Guinean *Tropidonophis*. Our SVDQuartets' tree shows a similar topology as Deepak *et al.* (2021), with *Tr. mairii* sister to *Tr. doriae*. But, as stated above, these two discrepancies are also the two nodes found with lowest nodal support within both StarBEAST and SVDQuartets. Thus, our species-tree inferences find the Australian representative's sister-taxon/taxa as being unresolved. Across all concatenated and species-tree inferences, the large terminal clade containing *Tr. mairii*, *Tr. doriae*, *Tropidonophis statisticus* Malnate and Underwood 1988, *Tropidonophis parkeri* Malnate and Underwood 1988, *Tropidonophis aenigmaticus* Malnate and Underwood 1988, and *Tr. multiscutellatus* has strong support, but contains short internal branches suggesting rapid radiation.

Divergence dating

Our phylogenies based on concatenated UCEs (75% completion matrix) and the 50 most-informative UCEs (95% completion matrix) were dated using treePL (Fig. 5; Supporting Information, Fig. S1) and StarBEAST (Fig. 4A), respectively. Dates for the treePL inferences are reported as 'date using Burbrink *et al.* (2019) calibration/date using Deepak *et al.* (2021) calibration'; also, see Table 2. The MRCA of *Tropidonophis* was found to be 13.6/18.2 and 9.7 (8.6–10.8) Mya, respectively. The Philippine clade was found to be 11.9/15.9 and 8.1 (6.9–9.4) Mya. New Guinean *Tropidonophis* was found to be 13.0/17.4 and 9.0 (7.8–10.3) Mya. In our treePL dated phylogenies using the two differing secondary node calibrations (Fig. 5; Supporting Information, Fig. S1), 9.2/12.4 Mya is the age of the MRCA of all mainland New Guinean species except *Tropidonophis dahlii* (Werner 1899), a Bismarck Archipelago endemic. For the remaining 10 New Guinean species of *Tropidonophis*, all cladogenic events occur from 9.2 to 4.4 (12.4–5.9) Mya. This difference in time is nearly the same as the divergence time between *Tr. dahlii* and this clade (~4/6 Mya), implying that mainland New Guinean *Tropidonophis* have speciated rapidly

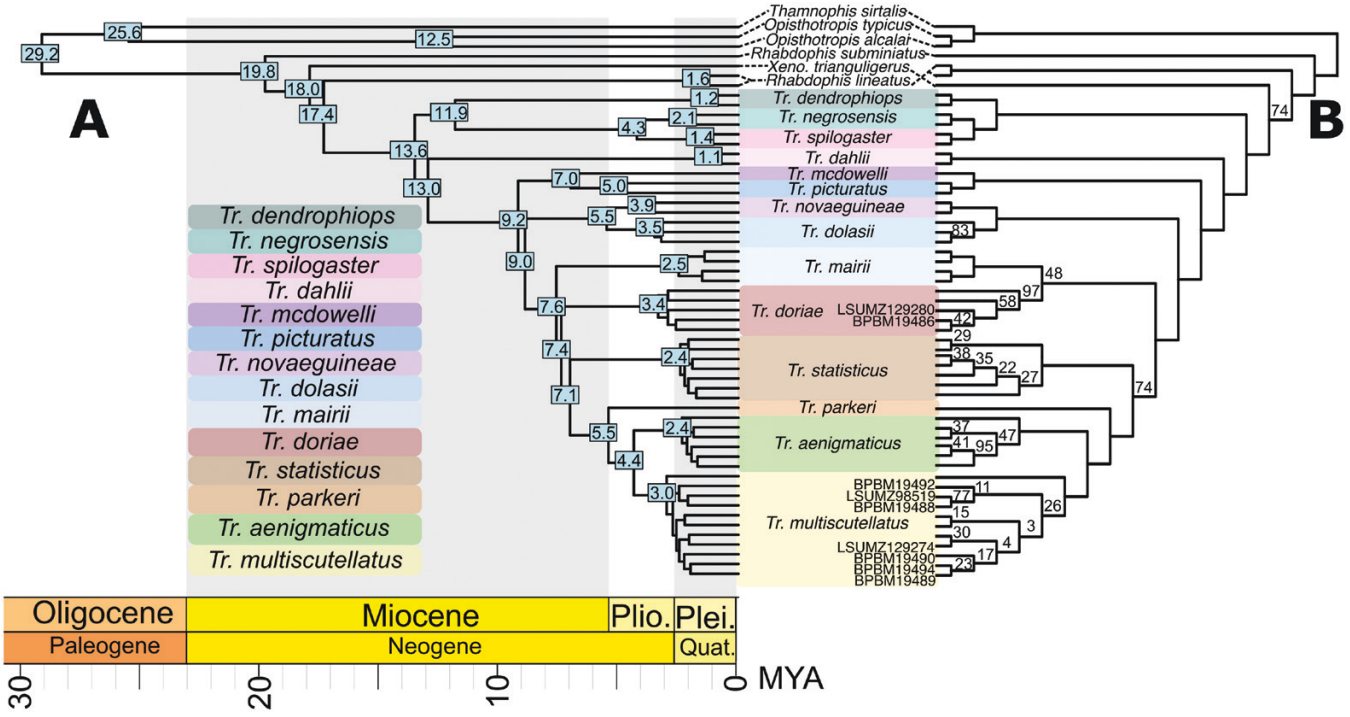

Figure 5. A,Ultrametric divergence-dated phylogeny of *Tropidonophis* inferred by treePL using Natricidae crown age from Burbrink *et al.* (2019); input topology was RAxML phylogeny (Fig. 3). Value at nodes is the mean age in million years. To maintain tree clarity, intraspecific nodal divergence estimates have not been included. B, species-tree estimation by SVDQuartets using the 'lineage tree' approach, which included all samples but with no a priori species identification (521 855 quartets). Catalogue numbers alongside tips indicate discordance with treePL tips in A. All node supports are 100 bootstrap support unless noted otherwise. The X-axis represents time in million years; Plio. = Pliocene, Plei. = Pleistocene, Quat. = Quaternary.

Table 2. Inferred divergence dates (in Mya) for major nodes from StarBEAST, treePL, and from Deepak *et al.* (2021). The treePL column contains two dates separated by slash: the left being the node estimate based on inference with the Burbrink *et al.* (2019) secondary node calibration for Natricidae (B-Age), and the right based on Deepak *et al.* (2021) secondary calibration (D-Age).

	StarBEAST	treePL (B-Age/D-Age)	treePL—Deepak *et al.* (2021)
***Tropidonophis* + SE Asian Natricid**	14.4 (12.8–16.0)	17.4/23.3	17.9
Tropidonophis	9.7 (8.6–10.8)	13.6/18.2	11.5
Philippine *Tropidonophis*	8.1 (6.9–9.4)	11.9/15.9	5.8
New Guinea *Tropidonophis*	9.0 (7.8–10.3)	13.0/17.4	11.3

relative to the earlier branching congenerics within a 6-million-year period and concurrently with the hypothesized maximum orogenic period of the Central Cordillera (Hall 2002, Quarles van Ufford and Cloos 2005). Within our StarBEAST results, we see a divergence time of almost 4 million years between the *Tr. dahlii* + mainland New Guinean *Tropidonophis* node [9.0 (7.8–10.3) Mya] and the MRCA of mainland New Guinean *Tropidonophis* [5.6 (5.0–6.3) Mya], again suggesting that mainland New Guinean *Tropidonophis* have speciated rapidly at the beginning of the Pliocene when compared to other congenerics within the phylogeny. This cladogenic timing coincides with the proposed Miocene-to-Pliocene orogeny of the Central Cordillera predicted in Hall (2002) and Quarles van Ufford and Cloos (2005). Inferred divergence dates for the four major nodes of focus in this work (*Tropidonophis* + sister SE Asian natricid, *Tropidonophis*, New Guinean *Tropidonophis*, Phiippine *Tropidonophis*) are strongly consistent with the treePL dates inferred for these same nodes in Deepak *et al.* (2021) (Table 2).

Ancestral biogeography

ModelTest within RASP found DEC+J to be the optimum biogeographic model for the concatenated treePLs [weighted AICc = 0.57, and 0.47 using calibration *sensu* Deepak *et al.* 2021 (Supporting Information, Table S1)] and 50 most-informative loci StarBEAST (weighted AICc = 0.65) chronograms (Table 3). DIVALIKE+J, although second to DEC+J, also received significant AICc weighting in both the treePL (0.39) and StarBEAST (0.31) ModelTest. Due to the AICc similarity between these two models, we inferred ancestral range estimations using both DEC+J (Fig. 7; Supporting Information, Fig. S2) and DIVALIKE+J (Supporting Information, Figs S3–S5). Biogeographic zones for phylogenies are reflected in Figure 6. Comparing our StarBEAST (Fig. 7A) to our treePL DEC+J range estimations (Fig. 7B; Supporting Information, Fig. S2), the MRCA of all *Tropidonophis* was present on the Oceanic Arc Terranes with a mean divergence date of 9.7 Mya during the Late Miocene, while the Mindanao PAIC was the estimated MRCA range within the treePL analyses with divergence dates of 13.6 (Fig. 7B) and 18.2 (Supporting Information, Fig. S2) Mya during the Mid-to-Early Miocene. For Philippine *Tropidonophis*, all estimations of biogeography found the MRCA to have ranged in the Luzon PAIC, the northern-most PAIC of the Philippine Islands. Between these two inferences, the treePL analysis appears more parsimonious and more logical. Under the StarBEAST hypothesized dispersal, the MRCA of all *Tropidonophis* reached the Oceanic Arc Terranes by the Mid-to-Late Miocene, but subsequently dispersed bidirectionally, backtracking north to the Luzon PAIC through the Mindanao PAIC, as well as south-east through to New Guinea. However, the treePL inference of a Mindanao PAIC distribution for the MRCA of all *Tropidonophis* suggests a much shorter dispersal north to the Luzon PAIC and continued south-east dispersal to the Oceanic Arc Terranes with no hypothesized backtracking through the Mindanao PAIC north to Luzon as suggested by the StarBEAST estimation (Fig. 7A). Range estimations under the DIVALIKE+J model were largely concordant with the DEC+J estimations for both input topology types, except for the DIVALIKE+J Deepak-date treePL estimation (Supporting Information, Fig. S4). In addition to different range estimation of the deeper two nodes (*R. subminiatus* + all tips; *X. trianguligerus* + all tips), the Deepak-dated treePL DIVALIKE+J estimation (Supporting Information, Fig. S4) placed the MRCA of all *Tropidonophis* in the Oceanic Arc Terranes, similar to both the DEC+J and DIVALIKE+J StarBEAST estimations (Fig. 7A; Supporting Information, Fig. S5). The StarBEAST ancestral range estimations (Fig. 7A; Supporting Information, Fig. S5) using the two different biogeographic models were concordant except for two internal nodes. Inference with the DEC+J model found the MRCA of *Tr. spilogaster* + *Tr. negrosensis* to range in the Luzon PAIC (PP = 0.55) while DIVALIKE+J found a probable range of both Mindoro + Negros-Panay PAIC (PP = 0.33). Inference with the DEC+J model found the MRCA of *Tr. dolasii* + *Tr. novaeguineae* to range in the Fold Belt and EPCT (PP = 0.71), while the DIVALIKE+J model found the EPCT (PP = 0.93) as the most probable ancestral range. Despite the differences between the inferences with DEC+J and DIVALIKE+J, both treePL-based range estimations using Burbrink *et al.* (2019) node calibration [DEC+J (Fig. 5), DIVALIKE+J (Supporting Information, Fig. S3)] and the DEC+J treePL with Deepak-dated calibration (Supporting Information, Fig. S2) appear to

Table 3. BioGeoBEARS ModelTest results for both input phylogenies from treePL and StarBEAST.

Input tree	Model	LnL	No. para.	D	E	J	AICc	AICc_wt
treePL	DEC+J	–46.54	3	0.0029	1.00E–12	0.073	100.9	0.57
	DIVALIKE+J	–46.94	3	0.0038	0.0009	0.05	101.7	0.39
	BAYAREALIKE+J	–49.16	3	0.0028	0.0038	0.18	106.2	0.042
	DIVALIKE	–54.63	2	0.012	0.02	0	114.1	0.0008
	DEC	–56.23	2	0.011	0.02	0	117.3	0.0002
	BAYAREALIKE	–61.02	2	0.029	0.093	0	126.9	1.30E–06
StarBEAST2	DEC+J	–40.14	3	0.0023	1.00E–12	0.1	88.13	0.65
	DIVALIKE+J	–40.87	3	0.0032	1.00E–12	0.063	89.59	0.31
	BAYAREALIKE+J	–42.94	3	0.0021	0.0068	0.17	93.73	0.039
	DIVALIKE	–49.5	2	0.019	0.028	0	103.8	0.0002
	DEC	–51.43	2	0.02	0.044	0	107.7	3.60E–05
	BAYAREALIKE	–56.44	2	0.044	0.14	0	117.7	2.40E–07

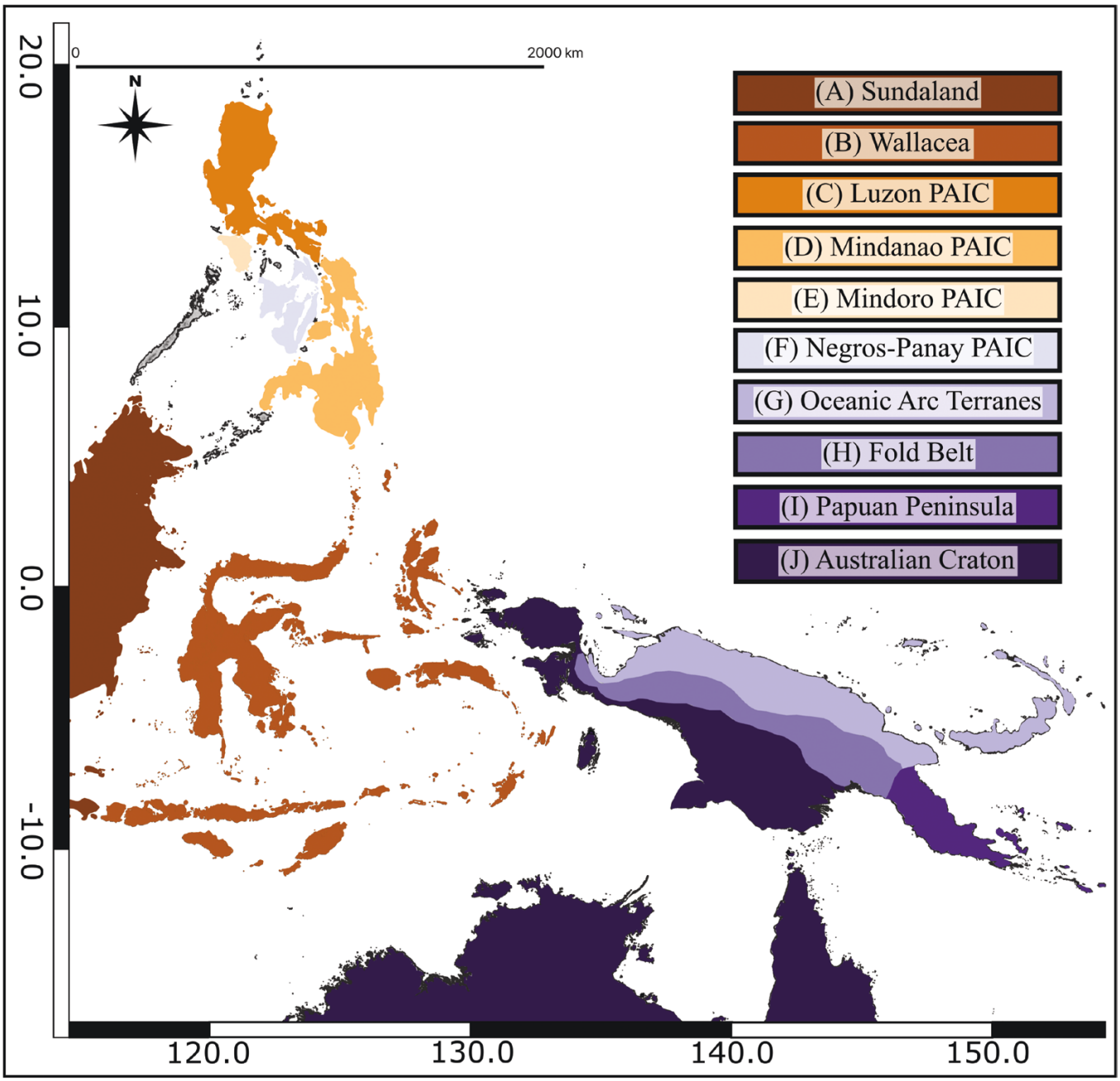

Figure 6. Pacific map showing the biogeographic realms used for ancestral-range estimation. Legend abbreviations are: PAIC, Pleistocene Aggregate Island Complexes; EPCT, East Papua Composite Terranes.

have more parsimonious dispersal histories since they suggest unidirectional dispersal north to south-east through to Australia and the EPCT. The MRCA of New Guinean *Tropidonophis* was found to have a most likely distribution on the Oceanic Arc Terranes. The MRCA of mainland New Guinean *Tropidonophis* sans *Tr. dahlii* across all the treePL and StarBEAST analyses was also a taxon found on the Oceanic Arc Terranes. For both StarBEAST and treePL, as one moves toward the most-terminal nodes, ranges shift from the Oceanic Arc Terranes to the Fold Belt, East Papua Composite Terrane, and one taxon (*Tr. mairii*) on the Australian Craton, suggesting a continued overall north to south-eastward dispersal for the genus from the Philippines to Australia.

DISCUSSION

The phylogenetics and biogeography of many New Guinean snake lineages have been evaluated using molecular-based sequence data (Austin 2000, Wüster *et al.* 2005, Williams *et al.* 2008, Austin *et al.* 2010, Metzger *et al.* 2010, Strickland *et al.* 2016, Ruane *et al.* 2018, Esquerré *et al.* 2020, 2021, 2022, Natusch *et al.* 2020, 2021, Roberts and Austin 2020, Deepak *et al.* 2021). Because of focused New Guinea field collecting and improvements in affordable target sequence capture, we have provided the most species-inclusive phylogenetic study for *Tropidonophis* using the most robust estimations of relatedness and biogeography due to thousands of nuclear loci. As we discuss above, our

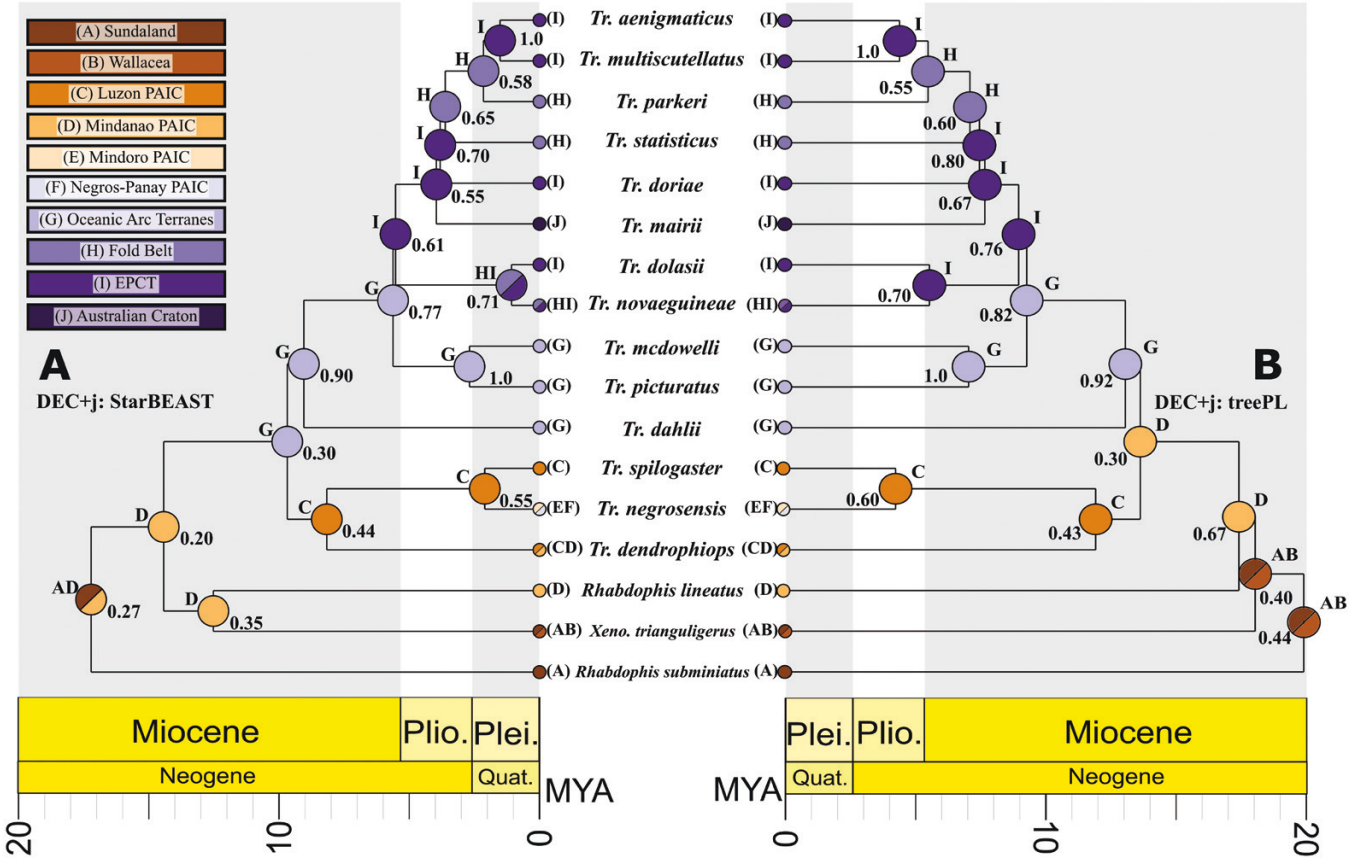

Figure 7. Ancestral-range estimation from BioGeoBEARS comparing trees and biogeographic hypotheses inferred by DEC+J on the (A) StarBEAST2 tree and (B) treePL phylogenies. Nodal-states indicated by letters aside node circles represent the most probable range estimation with the posterior probability of the range estimation denoted next to the node. Legend abbreviations are: PAIC, Pleistocene Aggregate Island Complexes; EPCT, East Papua Composite Terranes. The X-axis represents time in million years; Plio. = Pliocene, Plei. = Pleistocene, Quat. = Quaternary.

multiple analyses and datatypes produced phylogenies largely concordant with Deepak *et al.*'s (2021) study that included 11 species. Also, all phylogenies inferred here corroborated the placement of *Tr. spilogaster* and *Tr. negrosensis* as sister-species. Thus, we agree with the taxonomic reassignment of *Rhabdophis spilogaster* to *Tropidonophis sensu* Deepak *et al.* (2021). Malnate and Underwood (1988) inferred their phylogeny (Fig. 3B) based on 34 morphological characters, including traditional external scale counts, scale configurations, and detailed internal characters such as lung reduction and hemipenal morphology. Their monograph was truly a feat in terms of data collection and museum specimen science. It is difficult to make fine-scale comparisons between our results and Malnate and Underwood's (1988) dendrogram (Fig. 3B [Malnate and Underwood, 1988: fig. 33])] for two reasons: Malnate and Underwood's lack of phylogenetic resolution in their dendrogram and our absence of contemporary vouchers of Moluccan taxa for phylogenomics. Their dendrogram did infer the Philippine taxa as the earliest branching *Tropidonophis*, which is identical to our phylogenies; however, major discordance exists between our work and their monograph regarding the phylogenetic position of *Tr. doriae*, a mainland New Guinea taxon. Their monograph postulated *Tr. doriae* as sister to all other non-Philippine *Tropidonophis*. However, our phylogenies infer *Tr. doriae* as a late-branching lineage either sister to the Australian taxon, *Tr. mairii*, or nested within the mainland New Guinean clade. The reason for the early branching position within Malnate and Underwood's dendrogram is based primarily on two 'primitive' characters: count of posterior dorsal scale rows and degree of left lung reduction. *Tropidonophis doriae* has 17 dorsal scale rows past the midbody—a feature shared with *Tr. dahlii*, *Tr. dendrophiops*, *Tropidonophis hypomelas* (Günther 1877), and *Tr. negrosensis*—and has a left lung 'small with lumen and vascular walls', a character state shared with *Tr. dendrophiops* and *Tr. negrosensis*.

Only one species of *Tropidonophis* has been described since the Malnate and Underwood (1988) monograph: *Tropidonophis dolasii* (Kraus and Allison 2004). This species is endemic to the D'Entrecasteaux Archipelago, a chain of three islands north of the Papuan Peninsula at the eastern end of New Guinea (Fig. 2). The D'Entrecasteaux Archipelago hosts a second species of *Tropidonophis*, *Tr. aenigmaticus* (Malnate and Underwood 1988; type locality Fergusson Island—Fig. 2C). Our results found *Tropidonophis dolasii* and *Tropidonophis novaeguineae* as sister-species, the latter representing a mainland taxon found in the Fold Belt of the Central Cordillera as well as the EPCT (Figs 2–6). We also found *Tropidonophis aenigmaticus* sister to *Tr. multiscutellatus*, a taxon that we have sampled from PNG's Central Province on the EPCT. Compared to each other, *Tr.*

aenigmaticus and *Tr. dolasii* are not each other's closest relative. Rather than being sister-taxa, it appears more likely that wide-ranging and possibly sympatric MRCAs of *Tr. dolasii* + *Tr. novaeguineae* and *Tr. aenigmaticus* + *Tr. multiscutellatus* dispersed from the mainland source populations to the recently subaerial islands of the D'Entrecasteaux Archipelago. The dates of divergence inferred for these clades coincides with major tectonic changes in the Solomon Sea, specifically the splitting and spreading of the Solomon Sea seafloor, known as the Woodlark Rift (Weissel *et al.* 1982, Benyshek and Taylor 2021). The seafloor spreading of the Solomon Sea is still ongoing and is the fastest spreading seafloor known on earth (Ferris *et al.* 2006). Woodlark Rifting at the start of the Pliocene provided the mechanism needed for dispersal and speciation in this archipelago because it is thought to have been the event making the three islands of the D'Entrecasteaux Archipelago subaerial. The presence of metamorphic core complexes in this region of crustal extension exhumed the domal islands (Goodenough, Fergusson, and Normanby Islands) above the centre of the Woodlark Rift, making these islands subaerial and reachable via over-water dispersal ~4 Mya (Taylor *et al.* 1995, Baldwin *et al.* 2012, Miller *et al.* 2012, Webb *et al.* 2014, Kraus 2015). The D'Entrecasteaux Archipelago hosts interesting herpetofauna in addition to keelbacks, including both anuran and elapid endemics. Recent phylogenetics with these D'Entrecasteaux endemics find the same pattern we find within *Tropidonophis*, that D'Entrecasteaux endemic taxa are mostly sister to adjacent mainland lineages (Metzger *et al.* 2010, Oliver *et al.* 2013, Strickland *et al.* 2016, Kraus 2020, Roberts and Austin 2020, Hill *et al.* 2022).

An important difference between Malnate and Underwood's morphology-based phylogeny and biogeographic hypotheses and our sequence-based phylogenies is that we currently lack molecular data for the four Moluccan taxa [*Tropidonophis elongatus* (Jan 1865), *Tropidonophis halmahericus* (Boettger 1895), *Tropidonophis punctiventris* (Boettger 1895), and *Tropidonophis truncatus* (Peters 1863); Figs 2, 3]. Whether investigating phylogenetics or biogeography, inclusion of these taxa is critical for understanding the complete evolutionary history of this group, but the dearth of contemporary vouchers with associated tissues prevents their inclusion currently. Despite lacking these taxa, our hypothesized biogeographical findings strongly agree with Malnate and Underwood's (1988) five-stage dispersal pattern hypothesized for the genus. The stepping-stone model of gene flow is a pattern in phylogeography that assumes that gene flow only occurs between adjacent populations, creating a stair-like or stepping-stone branching pattern in phylogenies that corresponds lineages to geography; adjacent populations will be sister to each other, with the earliest branching lineage within the phylogeny representing the geographic origin of the group (Kimura 1953, Avise 2000, Yang *et al.* 2018). The stepping-stone model can also be applied as a mode of speciation. Within island systems, the stepping-stone model of speciation has been suggested as a testable alternative mode of lineage diversification relative to vicariance-driven allopatric speciation (Yang *et al.* 2018). The Sunda-Papuan keelbacks are an excellent system to continue testing lineage diversification via dispersal versus vicariance; however, our work suggests that dispersal and vicariance may not be mutually exclusive mechanisms when it comes to rapid radiations like *Tropidonophis*. Overall, the inferred trees suggest a stepping-stone model of dispersal, but the majority of cladogenetic events are found on the mainland of New Guinea beginning in the Pliocene.

Oceanic dispersal by way of rafting on vegetation mats has been the hypothesized dispersal mechanism for many squamate lineages (Austin 2000, Queiroz 2005, Yang *et al.* 2018). Squamates are proficient overwater dispersers compared to amphibians due to their integument's resistance to saline desiccation (Penner and Rödel 2019). Keelback snakes' proclivity for aquatic environments and aquatic vegetation may have facilitated rapid dispersal from Sunda to the Philippines, and south-eastward to the Oceanic Arc Terranes by way of vegetation mats (Fig. 7; Malnate and Underwood 1988). Across all our phylogenetic inferences, we find support for this dispersal pattern and, more specifically, a stepping-stone pattern of dispersal south-eastward towards the Sahul Shelf. However, regarding lineage diversification and species' diversity, dispersal does not appear to be the mechanism solely responsible for cladogenesis and species' richness in this genus. Half of the species' diversity (10 of 20) in *Tropidonophis* is found on mainland New Guinea, and two additional species are endemic to the Bismarck Archipelago (Fig. 2). Our data suggest *Tropidonophis* reached the Oceanic Arc Terranes in the Mid-Miocene roughly 15–10 Mya and, as the Pliocene approached, the Arc Terranes accreted with the northern margin of the Australian Plate, creating a significant orogenic event (that is still ongoing), pushing the Central Cordillera higher and continually reshuffling the north coast of New Guinea. Looking at all inferences together, this overall timing of dispersal and speciation supports both Hall's (2002) and Quarles van Ufford and Cloos' (2005) models. However, when evaluating the hypothetical logistics and most likely routes of dispersal for this group, and based on the data and analyses we produced, it seems more parsimonious that the biogeographic patterns predicted by our treePL inferences (Fig. 7B) are the likely route of dispersal, versus the backtracking from the Oceanic Arc Terranes to the Philippines predicted by the StarBEAST inferences (Fig. 7A). But this may be further clarified once the Moluccan taxa can be incorporated into our phylogeny. Interpreting together all cumulative divergence dating estimates, the 13–5 Mya period between the Miocene and the start of the Pliocene was a time of rapid diversification for *Tropidonophis* and the time of maximum terrane accretion from the island arc on the New Guinean mainland. Thus, probable rafting and utilization of stepping-stones permitted the Pacific Ocean range expansion for this lineage of natricids, but our analyses suggest that the accretion of the arc terranes and subsequent orogeny of the mainland provided the allopatry needed for rapid diversification and the species diversity that we see today.

CONCLUSIONS

We provide the most extensive analysis of phylogeny and historical biogeography for the Sunda-Papuan keelbacks. Our results agree with the previously inferred phylogenies that also used molecular sequence data (Deepak *et al.* 2021). We used multiple species-tree inference approaches never applied to this snake lineage and found strong support for all a priori species'

identifications made based on morphological examination, as well as congruence between species-trees and concatenated inferences. Biogeographically, our findings support the five-point hypothesis proposed by Malnate and Underwood (1988). While we performed robust and thorough estimations of biogeographic history, complete systematic and evolutionary history cannot be inferred until we have full coverage of the genus, specifically inclusion of the Moluccan taxa. While no ethanol-preserved tissues of these taxa are known to exist, methodologies for genomic sequence capture using formalin-fixed museum specimens are becoming increasingly more popular and successful (Ruane and Austin 2017, Bernstein and Ruane 2022). Until future expeditions can collect in these understudied islands, integrating formalin-fixed material may provide the key to elucidating these complicated systematic and evolutionary histories across New Guinean herpetofauna.

SUPPLEMENTARY DATA

Supplementary data are available at *Zoological Journal of the Linnean Society* online.

ACKNOWLEDGEMENTS

We first thank the two anonymous reviewers and handling editor whose constructive and thoughtful reviews bettered this work in many ways. For facilitation of fieldwork and access to the collections, we thank the entirety of the collection and curatorial staff at the Papua New Guinea National Museum and Art Gallery. For permission to work in PNG, we thank the PNG National Research Institute and the Department of Environment and Conservation (now the Conservation and Environmental Protection Authority), as well as the numerous governments of the provinces in which we worked. For aiding in collections, teaching us about local natural history, and generously hosting us, we thank the countless local naturalists and villagers of New Guinea. For insight into sample selection for Philippine taxa and ongoing work with *Rhabdophis*, we thank Rafe Brown and Jeff Weinell (University of Kansas Museum of Natural History). For assistance with analyses and data management we thank Justin Bernstein, Pamela Hart, Jessie Salter, Oscar Johnson, Anna Hiller, and Nelson Buainain Neto. For assistance with library preparations, we thank Zach Rodriguez. For performing some of the DNA extractions that were used in this study, we thank John Andermann (Louisiana State University Museum of Natural Sciences; LSUMNS). For commenting on this manuscript prior to submission, we thank J.R.R.'s Ph.D. graduate committee: Jacob Esselstyn, Brant Faircloth, and Ashley Long. For computing resources, we thank the CIPRES science gateway and the HPC at LSU. For processing loans for tissues used in this study, we thank Kelli DeLeon, Molly Hagemann, and Kenneth Hayes (Bernice P. Bishop Museum; BPBM), Ralph Foster and Sally South (Australian Biological Tissue Collection; ABTC), Rafe Brown and Luke Welton (University of Kansas Natural History Museum), Donna Dittman, Seth Parker, Fred Sheldon, and David Boyd (LSUMNS). For access to collections to gather morphometric data, we thank Frank Burbrink, David Kizirian, and Lauren Vonnahme (American Museum of Natural History) and Molly Hagemann. Tissues received from BPBM were collected during expeditions funded by grants DEB-0103794, DEB-0743890, and DEB-1145453 from the National Science Foundation, those received from KU were collected during expeditions funded by grants from the National Science Foundation DEB-0743491, DEB-1418895, DEB-1654388, and DEB-0344430 awarded to Rafe Brown. This work was funded by grants from the Coypu Foundation, National Geographic (NGS-53506R-18), National Science Foundation DEB-1146033 and DEB-1926783 to CCA, and National Science Foundation DEB-2224119 to S.R.. This is Contribution No. 2023-005 from Bishop Museum's Pacific Biological Survey.

CONFLICT OF INTEREST

The authors have no conflicts of interest associated with the work above.

DATA AVAILABILITY

The data underlying this article are available in the Dryad Digital Repository at https://dx.doi.org/10.5061/dryad.zw3r228f9.

REFERENCES

Aberer AJ, Kobert K, Stamatakis A. Exabayes: massively parallel bayesian tree inference for the whole-genome era. *Molecular Biology and Evolution* 2014;**31**:2553–6. https://doi.org/10.1093/molbev/msu236

Austin CC. Molecular phylogeny and historical biogeography of Pacific Island boas (*Candoia*). *Copeia* 2000;**2000**:341–52. https://doi.org/10.1643/0045-8511(2000)000[0341:mpahbo]2.0.co;2

Austin CC, Spataro M, Peterson S *et al*. Conservation genetics of Boelen's python (*Morelia boeleni*) from New Guinea: reduced genetic diversity and divergence of captive and wild animals. *Conservation Genetics* 2010;**11**:889–96. https://doi.org/10.1007/s10592-009-9931-z

Avise JC. *Phylogeography: The History and Formation of Species*. Boston: Harvard University Press, 2000.

Baldwin SL, Fitzgerald PG, Webb LE. Tectonics of the New Guinea region. *Annual Review of Earth and Planetary Sciences* 2012;**40**:495–520. https://doi.org/10.1146/annurev-earth-040809-152540

Bell MA, Lloyd GT. strap: an R package for plotting phylogenies against stratigraphy and assessing their stratigraphic congruence. *Palaeontology* 2015;**58**:379–89. https://doi.org/10.1111/pala.12142

Benyshek EK, Taylor B. Tectonics of the Papua-Woodlark Region. *Geochemistry, Geophysics, Geosystems* 2021;**22**:1–26.

Bernstein JM, Ruane S. Maximizing molecular data from specimens in natural history collections. *Frontiers in Ecology and Evolution* 2022;**10**:1–17.

Blair C, Bryson RW, Linkem CW *et al*. Cryptic diversity in the Mexican highlands: thousands of UCE loci help illuminate phylogenetic relationships, species limits and divergence times of montane rattlesnakes (Viperidae: *Crotalus*). *Molecular Ecology Resources* 2019;**19**:349–65. https://doi.org/10.1111/1755-0998.12970

Bolger AM, Lohse M, Usadel B. Trimmomatic: a flexible trimmer for Illumina sequence data. *Bioinformatics* 2014;**30**:2114–20. https://doi.org/10.1093/bioinformatics/btu170

Bouckaert R, Vaughan TG, Barido-Sottani J *et al*. BEAST 2.5: an advanced software platform for Bayesian evolutionary analysis. *PLoS Computational Biology* 2019;**15**:1–28.

Brown RM. Biogeography of vertebrates. *Encyclopedia of Evolutionary Biology* 2016;**1**:211–20.

Brown RM, Diesmos AC. Philippines, biology. In: Gillespie R, Clague D (eds.), *Encyclopedia of Islands*. Berkeley: University of California Press, 2009, 723–32.

Burbrink FT, Grazziotin FG, Pyron RA *et al*. Interrogating genomic-scale data for Squamata (Lizards, Snakes, and Amphisbaenians) shows no support for key traditional morphological relationships. *Systematic Biology* 2019;**69**:502–20. https://doi.org/10.1093/sysbio/syz062

Campbell MA, Buser TJ, Alfaro ME *et al*. Addressing incomplete lineage sorting and paralogy in the inference of uncertain salmonid phylogenetic relationships. *PeerJ* 2020;**8**:e9389–27. https://doi.org/10.7717/peerj.9389

Černy D. 2020. *Visualizing BEAST2 Time Trees*. Accessed 20 August 2021. https://davidcerny.github.io/post/plotting_beast/ (20 August 2021, date last accessed).

Chifman J, Kubatko L. Quartet inference from SNP data under the coalescent model. *Bioinformatics* 2014;**30**:3317–24. https://doi.org/10.1093/bioinformatics/btu530

Clouse RM, Giribet G. Across Lydekker's Line—first report of mite harvestmen (Opiliones: Cyphophthalmi: Stylocellidae) from New Guinea. *Invertebrate Systematics* 2007;**21**:207–27. https://doi.org/10.1071/is06046

Danecek P, Bonfield JK, Liddle J *et al*. Twelve years of SAMtools and BCFtools. *GigaScience* 2021;**10**:1–4.

Deepak V, Cooper N, Poyarkov NA *et al*. Multilocus phylogeny, natural history traits and classification of natricine snakes (Serpentes: Natricinae). *Zoological Journal of the Linnean Society* 2021;**195**:279–98. https://doi.org/10.1093/zoolinnean/zlab099

Del Fabbro C, Scalabrin S, Morgante M *et al*. An extensive evaluation of read trimming effects on illumina NGS data analysis. *PLoS One* 2013;**8**:e85024–13. https://doi.org/10.1371/journal.pone.0085024

Esquerré D, Donnellan S, Brennan IG *et al*. Phylogenomics, biogeography, and morphometrics reveal rapid phenotypic evolution in pythons after crossing Wallace's line. *Systematic Biology* 2020;**69**:1039–51.

Esquerré D, Donnellan SC, Pavón-Vázquez CJ *et al*. Phylogeography, historical demography and systematics of the world's smallest pythons (Pythonidae, *Antaresia*). *Molecular Phylogenetics and Evolution* 2021;**161**:107181. https://doi.org/10.1016/j.ympev.2021.107181

Esquerré D, Brennan IG, Donnellan S *et al*. Evolutionary models demonstrate rapid and adaptive diversification of Australo-Papuan pythons. *Biology Letters* 2022;**18**:20220360. https://doi.org/10.1098/rsbl.2022.0360

Faircloth BC. *Illumiprocessor: a Trimmomatic Wrapper for Parallel Adapter and Quality Trimming*. 2013. http://dx.doi.org/10.6079/J9ILL.

Faircloth BC. PHYLUCE is a software package for the analysis of conserved genomic loci. *Bioinformatics* 2016;**32**:786–8. https://doi.org/10.1093/bioinformatics/btv646

Faircloth BC. *itero*. 2018. https://github.com/faircloth-lab/itero.

Faircloth BC, McCormack JE, Crawford NG *et al*. Ultraconserved elements anchor thousands of genetic markers spanning multiple evolutionary timescales. *Systematic Biology* 2012;**61**:717–26. https://doi.org/10.1093/sysbio/sys004

Ferris A, Abers GA, Zelt B *et al*. Crustal structure across the transition from rifting to spreading: the Woodlark rift system of Papua New Guinea. *Geophysical Journal International* 2006;**166**:622–34. https://doi.org/10.1111/j.1365-246x.2006.02970.x

Flannery TF. 1990. *Mammals of New Guinea*. Carina, Queensland: Robert Brown and Associates.

Glenn TC, Nilsen RA, Kieran TJ *et al*. Adapterama I: universal stubs and primers for 384 unique dual-indexed or 147,456 combinatorially indexed Illumina libraries (iTru & iNext). *PeerJ* 2019;**7**:e7755–31. https://doi.org/10.7717/peerj.7755

Gradstein FM, Ogg JG, Hilgen FJ. On the geologic time scale. *Newsletters on Stratigraphy* 2012;**45**:171–88. https://doi.org/10.1127/0078-0421/2012/0020

Hall R. Cenozoic geological and plate tectonic evolution of SE Asia and the SW Pacific: computer-based reconstructions, model and animations. *Journal of Asian Earth Sciences* 2002;**20**:353–431. https://doi.org/10.1016/s1367-9120(01)00069-4

Hamilton WB. *Tectonics of the Indonesian Region. U.S. Geologic Survey Professional Paper 1078*. Washington, DC: U.S. Government Publishing Office, 1979. https://doi.org/10.3133/pp1078.

Hasegawa M, Kishino H, Yano T. Dating of the human-ape splitting by a molecular clock of mitochondrial DNA. *Journal of Molecular Evolution* 1985;**22**:160–74. https://doi.org/10.1007/bf02101694

Hill KC, Hall R. Mesozoic–Cenozoic evolution of Australia's New Guinea margin in a West Pacific context. *Special Paper of the Geological Society of America* 2003;**372**:265–90.

Hill EC, Fraser CJ, Gao DF *et al*. Resolving the deep phylogeny: implications for early adaptive radiation, cryptic, and present-day ecological diversity of Papuan microhylid frogs. *Molecular Phylogenetics and Evolution* 2022;**177**:107618. https://doi.org/10.1016/j.ympev.2022.107618

Hill EC, Gao DF, Polhemus DA *et al*. Testing geology with biology: plate tectonics and the diversification of microhylid frogs in the Papuan region. *Integrative Organismal Biology* 2023;**5**:obad028. https://doi.org/10.1093/iob/obad028

Holm RJ, Rosenbaum G, Richards SW. Post 8 Ma reconstruction of Papua New Guinea and Solomon Islands: microplate tectonics in a convergent plate boundary setting. *Earth-Science Reviews* 2016;**156**:66–81. https://doi.org/10.1016/j.earscirev.2016.03.005

Karin BR, Stubbs AL, Arifin U *et al*. Crossing Lydekker's line: Northern Water Dragons (*Tropicagama temporalis*) colonized the Mollucan Islands of Indonesia from New Guinea. *Herpetologica* 2020;**76**:344–50. https://doi.org/10.1655/herpetologica-d-19-00033

Katoh K, Standley DM. MAFFT multiple sequence alignment software v.7: improvements in performance and usability. *Molecular Biology and Evolution* 2013;**30**:772–80. https://doi.org/10.1093/molbev/mst010

Kimura M. 'Stepping stone' model of population. *Annual Report of the National Institute of Genetics, Japan* 1953;**3**:62–3.

Kraus F. A new species of the miniaturized frog genus *Paedophryne* (Anura: Microhylidae) from Papua New Guinea. *Occasional Papers of the University of Michigan Museum of Zoology* 2015;**745**:1–11.

Kraus F. A new species of *Toxicocalamus* (Squamata: Elapidae) from Papua New Guinea. *Zootaxa* 2020;**4859**:127–37.

Kraus F, Allison A. A new species of *Tropidonophis* (Serpentes: Colubridae: Natricinae) from the D'Entrecasteaux Islands, Papua New Guinea. *Proceedings of the Biological Society of Washington* 2004;**117**:303–10.

Leviton AE, Siler CD, Weinell JL *et al*. Synopsis of the snakes of the Philippines—a synthesis of data from biodiversity repositories, field studies, and the literature. *Proceedings of the California Academy of Sciences* 2018;**64**:399–568.

Li H, Durbin R. Fast and accurate short read alignment with Burrows–Wheeler transform. *Bioinformatics* 2009;**25**:1754–60. https://doi.org/10.1093/bioinformatics/btp324

Lydekker R. *A Geographical History of Mammals*. Cambridge: Cambridge University Press, 1896.

Malnate EV, Underwood G. Australasian natricine snakes of the genus *Tropidonophis*. *Proceedings of the Academy of Natural Sciences of Philadelphia* 1988;**140**:59–201.

Matzke NJ. Model selection in historical biogeography reveals that founder-event speciation is a crucial process in island clades. *Systematic Biology* 2014;**63**:951–70. https://doi.org/10.1093/sysbio/syu056

Matzke NJ. Statistical comparison of DEC and DEC+J is identical to comparison of two ClaSSE submodels, and is therefore valid. *Journal of Biogeography* 2022;**49**:1805–24. https://doi.org/10.1111/jbi.14346

Mayr E. Wallace's Line in light of recent zoogeographic studies. *The Quarterly Review of Biology* 1944;**19**:1–14. https://doi.org/10.1086/394684

Metzger GA, Kraus F, Allison A *et al*. Uncovering cryptic diversity in *Aspidomorphus* (Serpentes: Elapidae): evidence from mitochondrial and nuclear markers. *Molecular Phylogenetics and Evolution* 2010;**54**:405–16. https://doi.org/10.1016/j.ympev.2009.07.027

Miller MA, Pfeiffer W, Schwartz T. The CIPRES science gateway: a community resource for phylogenetic analyses. In: *Proceedings of the TeraGrid 2011 Conference: Extreme Digital Discovery, TG'11*, Utah: Salt Lake City, Utah, 2011 (18 July 2011, confrence held).

Miller SR, Baldwin SL, Fitzgerald PG. Transient fluvial incision and active surface uplift in the Woodlark rift of eastern Papua New Guinea. *Lithosphere* 2012;**4**:131–49. https://doi.org/10.1130/l135.1

Mirarab S, Reaz R, Bayzid S *et al*. ASTRAL: genome-scale coalescent-based species tree estimation. *Bioinformatics* 2014;**30**:541–8.

Natusch DJD, Esquerré D, Lyons JA *et al*. Species delimitation and systematics of the green pythons (*Morelia viridis* complex) of melanesia and Australia. *Molecular Phylogenetics and Evolution* 2020;**142**:106640. https://doi.org/10.1016/j.ympev.2019.106640

Natusch DJD, Esquerré D, Lyons JA *et al*. Phylogenomics, biogeography and taxonomic revision of New Guinean pythons (Pythonidae, Leiopython) harvested for international trade. *Molecular Phylogenetics and Evolution* 2021;**158**:106960. https://doi.org/10.1016/j.ympev.2020.106960

Ogilvie HA, Bouckaert RR, Drummond AJ. StarBEAST2 brings faster species tree inference and accurate estimates of substitution rates. *Molecular Biology and Evolution* 2017;**34**:2101–14. https://doi.org/10.1093/molbev/msx126

Oliver LA, Rittmeyer EN, Kraus F *et al*. Phylogeny and phylogeography of *Mantophryne* (Anura: Microhylidae) reveals cryptic diversity in New Guinea. *Molecular Phylogenetics and Evolution* 2013;**67**:600–7. https://doi.org/10.1016/j.ympev.2013.02.023

Paradis E, Claude J, Strimmer K. APE: Analyses of Phylogenetics and Evolution in R language. *Bioinformatics* 2004;**20**:289–90. https://doi.org/10.1093/bioinformatics/btg412

Penner J, Rödel MO. Keep it simple? Dispersal abilities can explain why species range sizes differ, the case study of West African amphibians. *Acta Oecologica* 2019;**94**:41–6. https://doi.org/10.1016/j.actao.2017.11.011

Pigram CJ, Davies HL. Terranes and the accretion history of the New Guinea orogen. *BMR Journal of Australian Geology & Geophysics* 1987;**10**:193–211.

Polhemus DA. Tectonic geology of Papua. In: Marshall AJ, Beehler BM (eds), *The Ecology of Indonesian Papua Part One*. Hong Kong: Periplus Editions, 2007, 137–64.

Prjibelski A, Antipov D, Meleshko D *et al*. Using SPAdes De Novo Assembler. *Current Protocols in Bioinformatics* 2020;**70**:1–29.

Quarles van Ufford A, Cloos M. Cenozoic tectonics of New Guinea. *American Association of Petroleum Geologists Bulletin* 2005;**89**:119–40.

Queiroz A de. The resurrection of oceanic dispersal in historical biogeography. *Trends in Ecology and Evolution* 2005;**20**:68–73.

Rambaut A, Drummond AJ, Xie D *et al*. Posterior summarization in Bayesian phylogenetics using Tracer 1.7. *Systematic Biology* 2018;**67**:901–4. https://doi.org/10.1093/sysbio/syy032

Ree RH, Sanmartin I. Conceptual and statistical problems with the DEC+J model of founder-event speciation and its comparison with DEC via model selection. *Journal of Biogeography* 2018;**45**:741–9. https://doi.org/10.1111/jbi.13173

Reynolds RG, Miller AH, Pasachnik SA *et al*. Phylogenomics and historical biogeography of West Indian Rock Iguanas (genus *Cyclura*). *Molecular Phylogenetics and Evolution* 2022;**174**:107548. https://doi.org/10.1016/j.ympev.2022.107548

Roberts JR, Austin CC. A new species of New Guinea Worm-Eating Snake (Elapidae: *Toxicocalamus* Boulenger, 1896), with comments on postfrontal bone variation based on micro-computed tomography. *Journal of Herpetology* 2020;**54**:446–59.

Roch S, Warnow T. On the robustness to gene tree estimation error (or lack thereof) of coalescent-based species' tree methods. *Systematic Biology* 2015;**64**:663–76. https://doi.org/10.1093/sysbio/syv016

Ruane S, Austin CC. Phylogenomics using formalin-fixed and 100+ year-old intractable natural history specimens. *Molecular Ecology Resources* 2017;**17**:1003–8. https://doi.org/10.1111/1755-0998.12655

Ruane S, Richards SJ, McVay JD *et al*. Cryptic and non-cryptic diversity in New Guinea ground snakes of the genus *Stegonotus* Duméril, Bibron and Duméril, 1854: a description of four new species (Squamata: Colubridae). *Journal of Natural History* 2018;**52**:917–44.

Salter JF, Oliveros CH, Hosner PA *et al*. Extensive paraphyly in the typical owl family (Strigidae). *Auk* 2020;**137**:1–15.

Simpson GG. Too many lines; the limits of the Oriental and Zoogeographic Regions. *Proceedings of the American Philosophical Society* 1977;**121**:107–20.

Slavenko A, Tamar K, Tallowin OJS *et al*. Cryptic diversity and non-adaptive radiation of montane New Guinea skinks (*Papuascincus*; Scincidae). *Molecular Phylogenetics and Evolution* 2020;**146**:106749. https://doi.org/10.1016/j.ympev.2020.106749

Smith SA, O'Meara BC. TreePL: divergence time estimation using penalized likelihood for large phylogenies. *Bioinformatics* 2012;**28**:2689–90. https://doi.org/10.1093/bioinformatics/bts492

Stamatakis A. RAxML v.8: a tool for phylogenetic analysis and post-analysis of large phylogenies. *Bioinformatics* 2014;**30**:1312–3. https://doi.org/10.1093/bioinformatics/btu033

Strickland JL, Carter S, Kraus F *et al*. Snake evolution in Melanesia: origin of the Hydrophiinae (Serpentes, Elapidae), and the evolutionary history of the enigmatic New Guinean elapid *Toxicocalamus*. *Zoological Journal of the Linnean Society* 2016;**178**:663–78. https://doi.org/10.1111/zoj.12423

Sukumaran J, Holder MT. DendroPy: a Python library for phylogenetic computing. *Bioinformatics* 2010;**26**:1569–71. https://doi.org/10.1093/bioinformatics/btq228

Swofford DL. *PAUP: Phylogenetic Analysis using Parsimony, v.4.0b10*. Sunderland: Sinauer Associates, 2003.

Tallowin OJS, Meiri S, Donnellan SC *et al*. The other side of the Sahulian coin: biogeography and evolution of Melanesian forest dragons (Agamidae). *Biological Journal of the Linnean Society* 2020;**129**:99–113. https://doi.org/10.1093/biolinnean/blz125

Taylor B, Goodliffe A, Martinez F *et al*. Continental rifting and initial sea-floor spreading in the Woodlark basin. *Nature* 1995;**374**:534–7. https://doi.org/10.1038/374534a0

Toussaint EFA, Hall R, Monaghan MT *et al*. The towering orogeny of New Guinea as a trigger for arthropod megadiversity. *Nature Communications* 2014;**5**:4001. https://doi.org/10.1038/ncomms5001

Unmack PJ, Allen GR, Johnson JB. Phylogeny and biogeography of rainbowfishes (Melanotaeniidae) from Australia and New Guinea. *Molecular Phylogenetics and Evolution* 2013;**67**:15–27. https://doi.org/10.1016/j.ympev.2012.12.019

Wallace AR. Notes of a voyage to New Guinea. *Journal of the Royal Geographical Society of London* 1860;**30**:172–7. https://doi.org/10.2307/1798299

Wascher M, Kubatko L. Consistency of SVDQuartets and maximum likelihood for coalescent-based species' tree estimation. *Systematic Biology* 2021;**70**:33–48. https://doi.org/10.1093/sysbio/syaa039

Webb LE, Baldwin SL, Fitzgerald PG. The Early–Middle Miocene subduction complex of the Louisiade Archipelago, southern margin of the Woodlark Rift. *Geochemistry, Geophysics, Geosystems* 2014;**15**:4024–46. https://doi.org/10.1002/2014gc005500

Weijola V, Vahtera V, Lindqvist C *et al*. A molecular phylogeny for the Pacific monitor lizards (*Varanus* subgenus *Euprepiosaurus*) reveals a recent and rapid radiation with high levels of cryptic diversity. *Zoological Journal of the Linnean Society* 2019;**186**:1053–66. https://doi.org/10.1093/zoolinnean/zlz002

Weissel JK, Taylor B, Karner GD. The opening of the Woodlark Basin, subduction of the Woodlark spreading system, and the evolution of Northern Melanesia since mid-Pliocene time. *Tectonophysics* 1982;**87**:253–77. https://doi.org/10.1016/0040-1951(82)90229-3

Williams DJ, O'Shea M, Daguerre RL *et al*. Origin of the eastern brownsnake, *Pseudonaja textilis* (Duméril, Bibron and Duméril) (Serpentes: Elapidae: Hydrophiinae) in New Guinea: evidence of multiple dispersals from Australia, and comments on the status of *Pseudonaja textilis pughi* Ho. *Zootaxa* 2008;**1703**:47–61.

Wüster W, Dumbrell AJ, Hay C *et al*. Snakes across the Strait: trans-Torresian phylogeographic relationships in three genera of Australasian snakes (Serpentes: Elapidae: *Acanthophis*, *Oxyuranus*, and *Pseudechis*). *Molecular Phylogenetics and Evolution* 2005;**34**:1–14. https://doi.org/10.1016/j.ympev.2004.08.018

Yang SF, Komaki S, Brown RM *et al*. Riding the Kuroshio Current: stepping stone dispersal of the Okinawa tree lizard across the East Asian Island Arc. *Journal of Biogeography* 2018;**45**:37–50. https://doi.org/10.1111/jbi.13111

Yu Y, Blair C, He X. RASP 4: ancestral state reconstruction tool for multiple genes and characters. *Molecular Biology and Evolution* 2020;**37**:604–6. https://doi.org/10.1093/molbev/msz257

Zaher H, Murphy RW, Arredondo JC *et al*. Large-scale molecular phylogeny, morphology, divergence-time estimation, and the fossil record of advanced caenophidian snakes (Squamata: Serpentes). *PLoS One* 2019;**14**:e0216148. https://doi.org/10.1371/journal.pone.0216148

Zhang C, Rabiee M, Sayyari E *et al*. ASTRAL-III: polynomial time species' tree reconstruction from partially resolved gene trees. *BMC Bioinformatics* 2018;**19**:15–30.